



1 **A Hydrologic Monitoring Dataset for Food and Water Security** 2 **Applications in Central Asia**

3 Amy L. McNally^{1,2,3}, Jossy Jacob^{1,4}, Kristi Arsenault^{1,2}, Kimberly Slinski^{1,5}, Daniel P. Sarmiento^{1,2},
4 Andrew Hoell⁶, Shahriar Pervez⁷, James Rowland⁸, Mike Budde⁸, Sujay Kumar¹, Christa Peters-
5 Lidard¹, James P. Verdin³

6
7 1 NASA Goddard Space Flight Center, Greenbelt, MD, 20771, United States

8 2 SAIC, Reston, VA, 20190, United States

9 3 United States Agency for International Development, Washington, DC, 20523, United States

10 4 SSAI, Inc., Lanham, MD, postal code, United States

11 5 University of Maryland Earth Systems Science Interdisciplinary Center, College Park, MD,
12 20740, United States

13 6 National Oceanic and Atmospheric Administration, Physical Science Laboratory, Boulder, CO,
14 80305, United States

15 7 Arctic Slope Regional Corporation (ASRC) Federal Data Solutions, Contractor to U.S. Geological
16 Survey, Earth Resources Observation and Science Center (EROS), Sioux Falls, SD, 57198 United
17 States

18 8 United States Geological Survey, EROS Center, Sioux Falls, South Dakota, 57198, United States

19

20 *Correspondence to:* Amy L. McNally (amy.l.mcnally@nasa.gov)

21



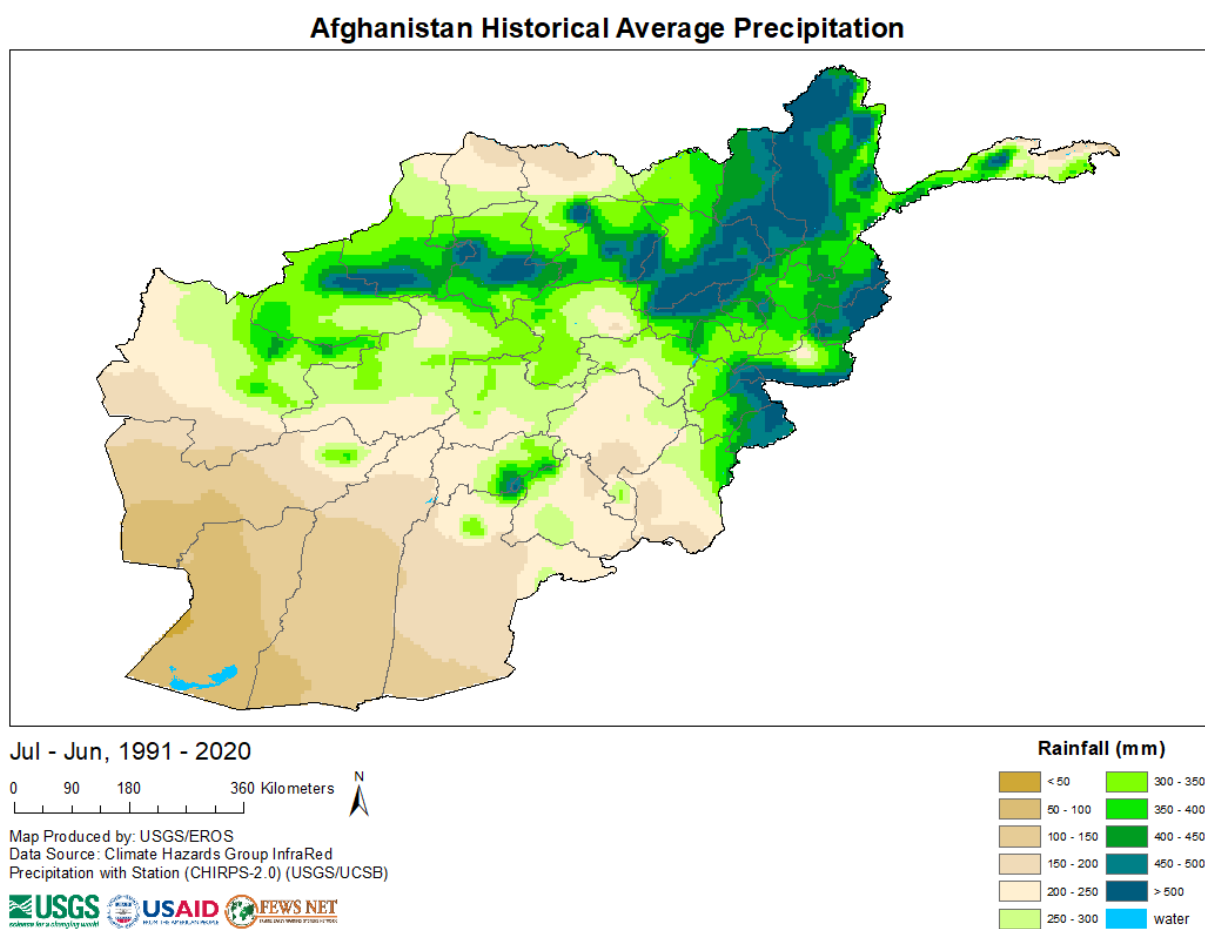
22 **Abstract**

23
24 From the Hindu Kush Mountains to the Registan desert, Afghanistan is a diverse landscape where
25 droughts, floods, conflict, and economic market accessibility pose challenges for agricultural
26 livelihoods and food security. The ability to remotely monitor environmental conditions is critical to
27 support decision making for humanitarian assistance. The FEWS NET Land Data Assimilation
28 System (FLDAS) global and Central Asia data streams described here combine meteorological
29 reanalysis datasets and land surface models to generate routine estimates of snow-covered fraction,
30 snow water equivalent, soil moisture, runoff and other variables representing the water and energy
31 balance. This approach allows us to fill the gap created by the lack of in situ hydrologic data in the
32 region. First, we describe the configuration of the FLDAS and the two resultant data streams: one,
33 global, at ~1 month latency, provides monthly average outputs on a 10 km² grid from 1982-present.
34 The second data stream, Central Asia, at ~1 day latency, provides daily average outputs on a 1 km²
35 grid from 2001-present. We describe our verification of these data that are compared to other
36 remotely sensed estimates as well as qualitative field reports. These data and value-added products
37 (e.g., anomalies and interactive time series) are hosted by NASA and USGS data portals for public
38 use. The global data stream with a longer record, is useful for exploring interannual variability,
39 relationships with atmospheric-oceanic teleconnections (e.g., ENSO), trends over time, and
40 monitoring drought. Meanwhile, the higher spatial resolution Central Asia data stream, with lower
41 latency, is useful for simulating snow-hydrologic dynamics in complex topography for monitoring
42 snowpack and flood risk.



43 1 Introduction

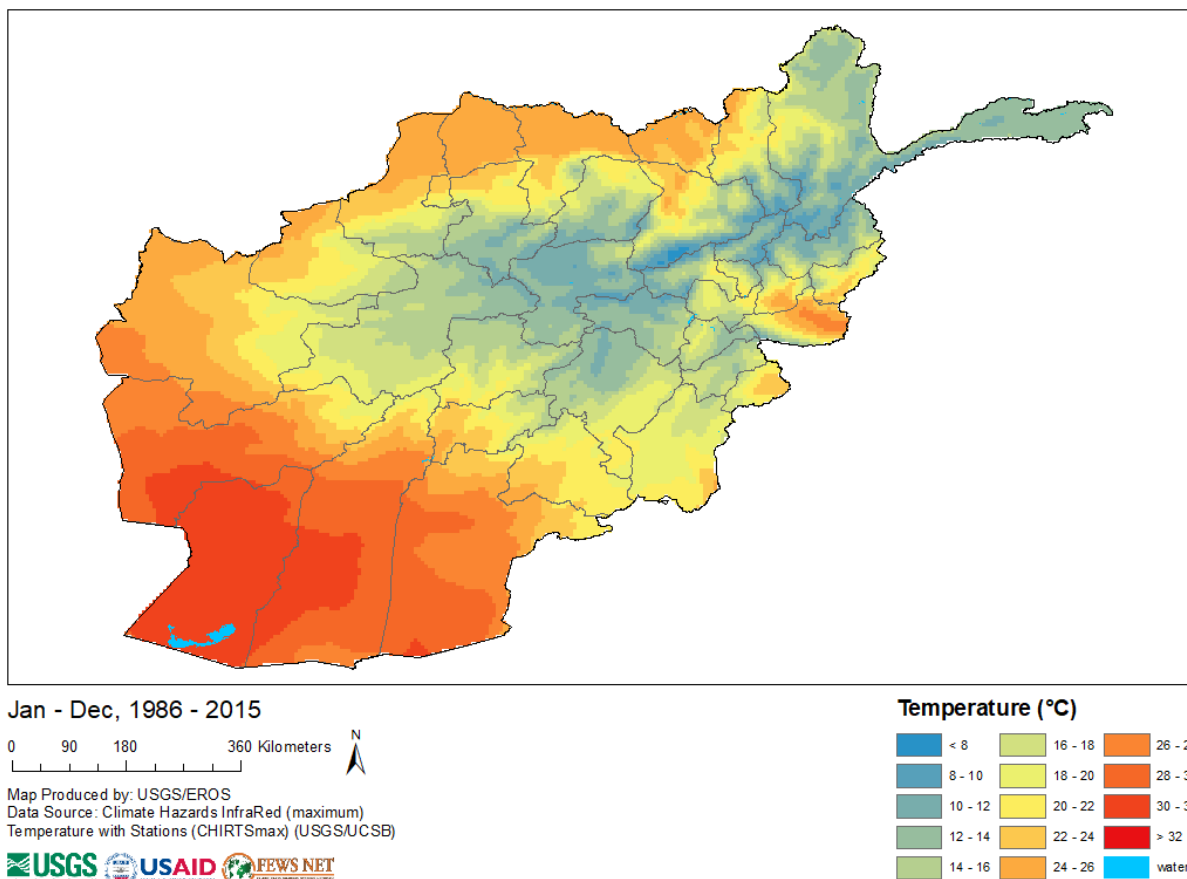
44 1.1 Central Asia Weather and Climate



45
46 Figure 1a. Mean annual precipitation in Afghanistan from 1991-2020, overlaid on province
47 boundaries. Map (USGS Knowledge Base, 2021) with data from Funk et al. (2015).



Afghanistan Historical Average Maximum Temperature



48
49 Figure 1b. Average maximum monthly temperature from (1986-2015), overlaid on province
50 boundaries. Map (USGS Knowledge Base, 2021) with data from Verdin et al. (2020).
51

52 Central Asia, a region that includes Afghanistan, is water-scarce receiving roughly 75% of its
53 annual precipitation during November–April (Oki and Kanae, S., 2006). In Afghanistan, rainfall is
54 highest in the northeast Hindu Kush Mountains and decreases toward the arid southwest Registan
55 Desert (Fig. 1a). Temperature follows a similar pattern with cooler temperatures in the high
56 elevation and wetter northeast and warmer temperature in the south, and southwest (Fig. 1b).
57 Regional precipitation is strongly influenced by the El Niño-Southern Oscillation (ENSO). La Niña
58 condition are associated with below average precipitation (FEWS NET, 2020b) and El Niño
59 conditions associated with above average precipitation (Barlow et al., 2016; Hoell et al., 2017; Rana
60 et al., 2018; Hoell et al., 2018, 2020; FEWS NET, 2020a). Other dynamical factors with an
61 important influence on precipitation include orography, storm tracks, and the Madden–Julian
62 oscillation (MJO) (Barlow et al., 2005; Nazemosadat and Ghaedamini, 2010; Hoell et al., 2018).
63 The last several years have experienced a number of ENSO events, with recent La Niña events in

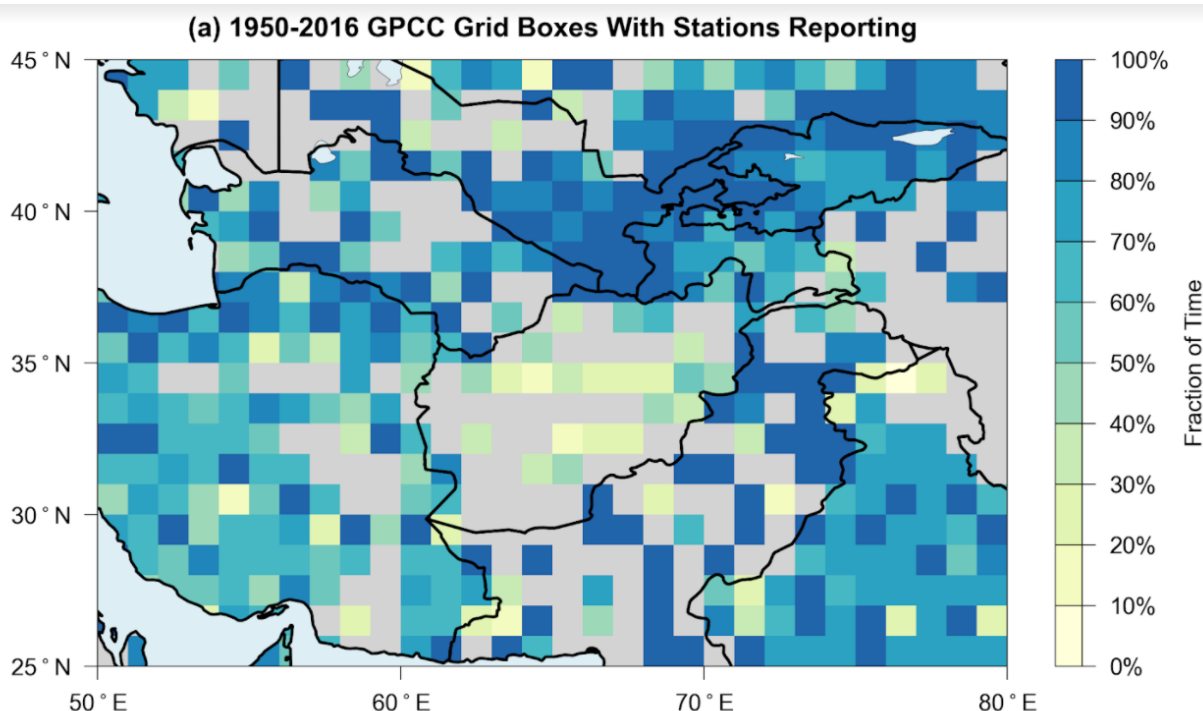


64 2016-17, 2017-18, and 2020-2021 (NOAA CPC ENSO Cold & Warm Episodes by Season, 2021)
65 that corresponded to droughts (FEWS NET, 2017b, 2018c, 2021).

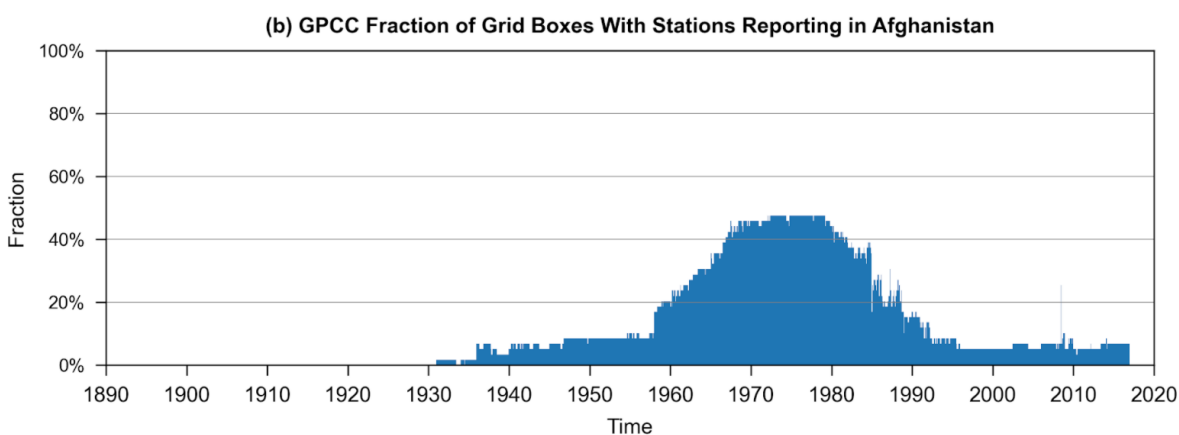
66
67 Despite Afghanistan's semi-arid climate, agriculture is an important sector, contributing 23% of the
68 gross domestic product and employing 44% of the national labor force (CIA World Factbook). High
69 mountain snowpack and snowmelt runoff are important for agricultural water supply, and according
70 to the Famine Early Warning Systems Network (FEWS NET, 2018b) is responsible for "providing
71 over 80% of irrigation water used. The timing and duration of the snowmelt is a key factor in
72 determining the volume of irrigation water and the length of time that it is available, as well as its
73 availability for use in marginal areas that experience [variable] rainfall." Therefore, routine
74 hydrologic monitoring, with a particular emphasis on snow, is critical for tracking agricultural
75 conditions and provides early warning for food insecurity.

76 **1.2 Precipitation Data Availability in Afghanistan**

77 Sparse in-situ precipitation observations lead to uncertainty in gridded and satellite-based
78 precipitation estimates which are important for environmental monitoring and driving hydrologic
79 models. Precipitation station observations are used for (a) bias correction of satellite estimates and
80 (b) validation of gridded products. In terms of gridded dataset development, Hoell et al. (2015)
81 describe lack of station observations in Afghanistan, Iraq and Pakistan and how complex
82 topography in these locations makes this issue particularly problematic. Barlow et al. (2016) also
83 highlight the station availability across the region and how that influences uncertainties in the
84 Global Precipitation Climatology Center (GPCC) version 6 dataset over Central Asia (Fig. 2a) and
85 specifically Afghanistan over time (Fig. 2b). Related to validation, Yoon et al. (2019) highlight that
86 the representativeness of the sparse in-situ data is a serious limitation in their evaluation of
87 precipitation over High Mountain Asia.
88



89



90

91 Figure 2. a) Station data availability underlying the GPCC version 6 dataset, for the 1951–2010
92 period, on the 0.5°-resolution grid over Central Asia. b) Number of Stations used as input to GPCC
93 rainfall dataset in Afghanistan.

94

95 Despite uncertainties, Schiemann et al. (2008) find that gridded precipitation estimates can
96 qualitatively identify large scale spatial distribution of precipitation, seasonal cycle and interannual
97 variability (i.e., wet and dry years) across Central Asia. Long term estimates of rainfall from satellite
98 derived products, as well as derived historic time series from hydrologic modelling, can be used as a
99 baseline of “observations,” from which we can have a sense of relative conditions, i.e., anomalies



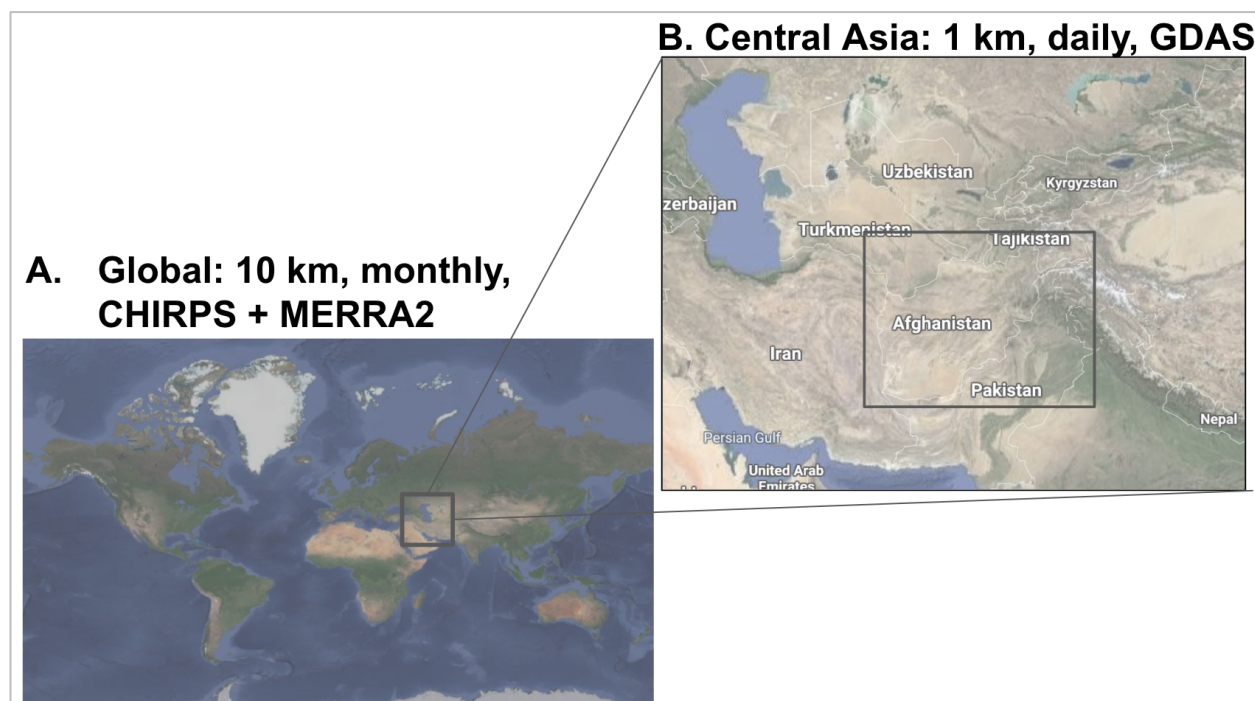
100 and variability. When this historical record is harmonized with a routine monitoring system, current
101 conditions can be placed in historical context. Anomaly-based representation of hydrologic
102 extremes can provide confidence in modeled estimates that have the potential to influence
103 agricultural, water resources and food security outcomes.

104
105 In addition to reliance on the representation of relatively wet and dry conditions, a “convergence of
106 evidence” approach that draws on (quasi-)independent sources of information is useful to
107 understand actual conditions. For convergence of Earth observations, hydrologic models can
108 generate ensembles of historic, current or future estimates of snow, streamflow, soil moisture, and
109 evapotranspiration which can then be compared to satellite derived estimates of surface water (e.g.
110 McNally et al., 2019), soil moisture (e.g. McNally et al., 2016), vegetation conditions and
111 evapotranspiration (e.g. Pervez et al., 2021; Jung et al., 2019), snow cover (e.g. Arsenault et al.,
112 2014), in situ stream flow (e.g. Jung et al., 2017) and others. Hydrologic estimates can also be
113 compared to outcomes in crop production e.g. (McNally et al., 2015; Davenport et al., 2019; Shukla
114 et al., 2020), and nutrition, health, and food security (e.g. Grace and Davenport, 2021) to provide a
115 qualitative understanding of both hydrologic model performance and conditions on the ground. In
116 this paper we provide an example of 2018 where drought conditions were associated with crisis
117 levels of acute food insecurity over most of Afghanistan (FEWS NET, 2018c).

118
119 This paper describes the FLDAS hydrologic modeling system’s global and Central Asia data
120 streams, which are designed for food and water security applications. These data streams provide a
121 long historic record for contextualizing estimates, as well as low latency data for timely decision
122 support. These data streams can also support research and monitoring by the broader food and water
123 security community. The purpose of this data descriptor is four-fold: (1) describe the development
124 of the moderate resolution, low latency FLDAS system to inform hydrologic monitoring for Central
125 Asia, specifically Afghanistan, (2) increase awareness of these data resources which are intended to
126 be a public good, (3) demonstrate how our methods inform critical investigations that ultimately
127 improve general understanding of water resources in this important region of the world, and (4)
128 advocate for a convergence of evidence approach to hydrologic monitoring in locations where all
129 sources of information contain some level of uncertainty. An outline of this data descriptor is as
130 follows. First, in the Methods (section 2) we describe the hydrologic modeling system, parameters
131 and meteorological inputs and model outputs. In the Results (section 3) we report comparisons to
132 other precipitation estimates, as well as comparisons of modeled snow estimates to remotely sensed
133 snow observations and find generally good agreement. Finally, we describe an application (section
134 4) of these data to the Afghanistan drought of 2018.



135 2 Methods



136
137 Figure 3. The FEWS NET Land Data Assimilation System (FLDAS) domains for (A) the global
138 data stream at 10 km² spatial resolution, and ~1 month latency for monthly averaged hydrologic
139 estimates and (B) the Central Asia data stream at 1 km² spatial resolution and ~1 day latency for
140 daily averaged hydrologic estimates. Imagery 2021 TerraMetrics, Map data © Google.

141 2.1 Land Surface Modeling System & Parameters

142 Land surface models (LSMs) can provide spatially and temporally continuous information about the
143 water and energy budgets of the land surface. This information is useful for food and water security
144 applications in places where in situ measurements of rainfall, soil moisture, snow and runoff are
145 sparse. This is particularly relevant in mountainous places like Afghanistan where heterogeneous
146 geography limits the representativeness of sparse in situ measurements. We use NASA's Land
147 Information System Framework (LISF), which is comprised of a pre-processor, the Land Data
148 Toolkit (Arsenault et al., 2018), the Land Information System (Kumar et al., 2006; Peters-Lidard et
149 al., 2007), and the Land Verification Toolkit (Kumar et al., 2012). To support the needs of FEWS
150 NET we have developed a custom instance of the NASA LISF - the FEWS NET Land Data
151 Assimilation System (FLDAS) (McNally et al., 2017). In this data descriptor we describe the two
152 configurations of the FLDAS data streams used for Central Asia food and water security
153 applications. It uses the Noah 3.6 Land Surface Model (Chen et al., 1996; Ek et al., 2003) and has
154 two data streams. One, global, at ~1 month latency, provides monthly average outputs on a 10 km²
155 grid from 1982-present. The second data stream, Central Asia, ~1 day latency, provides daily



156 average outputs at 1 km² from 2001-present. While the two data stream specifications are largely the
 157 same, there are some differences related to the input parameters and specifications (Table 1) and
 158 model spin-up procedure.

159

160 Table 1. FEWS NET Land Data Assimilation System (FLDAS) specifications for (A) global data
 161 stream, 10 km², monthly with CHIRPS+MERRA-2. (B) Central Asia data stream 1 km² daily with
 162 GDAS.

	Global	Central Asia
Spatial Extent	179.95°W- 179.95°E, 59.95°S-89.95°N	30-100°E, 21-56°N
Landmask	Land Data Toolkit (LDT) generated from MODIS (Arsenault et al. 2018)	MOD44w (Carroll et al., 2017)
Landcover	IGBP landcover	IGBP landcover
Parameters	FAO Soils Reynolds et al (2000)	FAO Soils
Elevation	SRTM (NASA JPL, 2013)	SRTM
Albedo	NCEP albedo (Csiszar, I., and Gutman 1999)	NCEP albedo
Albedo	Native Max Snow Albedo; Barlage (2005)	Native Max Snow Albedo
Vegetation Parameters	NCEP greenness fraction (Gutman and Ignatov 1997)	NCEP greenness fraction
Non-Precipitation Meteorological Inputs	MERRA-2 meteorological variables	GDAS meteorological variables
Soil Texture	FAO STATSGO soil texture	FAO STATSGO soil texture
Precipitation Inputs	CHIRPS daily precipitation, downscaled to 3-hourly with LDT	GDAS 3-hourly precipitation
Specifications	Noah 3.6.1	Noah 3.6.1
Map Projection	Geographic Latitude-Longitude	Geographic Latitude-Longitude
Software Version	7.2	7.3
Spatial Resolution	0.1 degree	0.01 degree
Temporal Coverage	1982-01-01 to present	2001-10-01 to present
Model Timestep	30-min timestep	15-min timestep



Met. Forcing Heights	2m Air Temperature (Tair), 10m Wind	2m Tair, 10m Wind
Soil layers (meters)	0-0.1; 0.1-0.4; 0.4-1.0; 1-2	0-0.1; 0.1-0.4; 0.4-1.0; 1-2
Features	radiation correction	radiation correction

163
164 The parameters and specifications listed in Table 1 are largely default settings defined by the Noah
165 LSM community (NCAR Research Applications Library, 2021). One important feature, added by
166 the NASA LISF software development team, is the radiation correction described in Kumar et al.
167 (2013), which improves the representation of snow dynamics with respect to slope and aspect
168 corrections on the downward solar radiation field. The precipitation and other meteorological
169 forcing variables, the period of record, and the spatial resolution were all determined to best meet
170 the target end-users' needs (i.e. FEWS NET) for routine agricultural and hydrologic monitoring.
171

172 Another noteworthy feature is the method of the Central Asia data stream restart (i.e., annual
173 initialization based on climatology), which was developed to address an issue of excessive inter-
174 annual snow accumulation found in the Noah LSM. First, a nine-year spin-up of the system was
175 performed to produce stable snow and soil moisture conditions. Next, the resulting model states
176 were compared with the Moderate Resolution Imaging Spectroradiometer (MODIS) Maximum
177 Snow Extent data originally computed by NOAA National Operational Hydrologic Remote Sensing
178 Center (Personal Communication Greg Fall, 2014). Then, the model estimated conditions were
179 adjusted to produce a climatological model state for 1 October that is used to initialize each year.
180 This approach ensures that the 'water year', beginning 1 October, is initialized with a reasonable
181 amount of snowpack. While this method does effectively manage excessive inter-annual snow
182 accumulation, the user should be aware that using the climatological model state will persist for ~1-
183 2 months in the water and energy balance of the LSM until they are superseded by "observed"
184 meteorological inputs for the current water year. Preliminary work indicates that this issue will be
185 resolved in future updates. In contrast, the global data stream does not employ this 1 October
186 initialization procedure.

187 **2.2 Meteorological Forcing Inputs**

188 Precipitation is the most important input to the FLDAS products. The lower-latency Central Asia
189 data stream is a daily product, forced with NOAA's Global Data Assimilation System (GDAS)
190 (Derber et al., 1991) 3-hourly precipitation, which is available from 2001-present at <1-day latency.
191 Meanwhile, the global data stream is driven by the daily CHIRPS precipitation product, which is
192 available from 1981 present at ~5-day latency for CHIRPS Preliminary and ~1.5-month latency for
193 CHIRPS Final. As mentioned earlier, lack of rainfall stations for bias correction of satellite-derived
194 estimates and evaluation poses a major challenge. However, we find that the GDAS rainfall product
195 and the CHIRPS rainfall product are adequate for routine monitoring and, along with additional
196 sources of remote sensed information, important for convergence of evidence when making a best
197 guess at land surface states and fluxes.



198
199 Before the daily CHIRPS rainfall can be used as input to the FLDAS models, the daily precipitation
200 must be pre-processed to a sub-daily timestep, using the LDT component of the LIS software. LDT
201 temporally disaggregates the daily CHIRPS rainfall, using an approach similar to the North
202 American LDAS precipitation downscaling method (Cosgrove et al., 2003). For this approach, we
203 use a finer timescale MERRA-2 precipitation as a reference dataset to represents an accurate diurnal
204 cycle. Coarser scale meteorological forcings are spatially disaggregated to the output resolution
205 (0.01, and 0.1 degree for Central Asia and global, respectively) in the LIS using bilinear
206 interpolation.

207
208 The FLDAS models require additional meteorological inputs, including air temperature, humidity,
209 radiation, and wind. The lower-latency Central Asia data stream uses GDAS 3-hourly
210 meteorological inputs available from 2001-present at <1-day latency. For a longer historical record,
211 the global data stream of FLDAS uses NASA's Modern Era Reanalysis for Research and
212 Applications version 2 (MERRA-2) (Gelaro et al., 2017) (1979-present) 1-hourly products with a
213 two-week latency.

214 **2.3 Model Evaluation Statistics and Comparison Data**

215 To assess the quality of our modeling outputs, we conduct comparisons between (1) FLDAS
216 satellite rainfall inputs and other satellite precipitation estimates, and (2) model estimated snow
217 cover fraction and satellite derived snow cover fraction estimates.

218
219 For the precipitation analysis, we compare CHIRPS and GDAS inputs to the Integrated Multi-
220 satellite Retrievals for the Global Precipitation Mission (IMERG), a NASA precipitation product
221 that integrates passive microwave and infrared satellite data with surface station observations
222 (Huffman et al., 2020). The IMERG Final Run precipitation product, available at ~ 2-month latency
223 (thus not suitable for our monitoring applications) has been used in numerous verification studies,
224 including studies over Africa (Dezfuli et al., 2017), South America (Gadelha et al., 2019; Manz et
225 al., 2017) and the mid-Atlantic region of the United States (Tan et al., 2016). These studies
226 demonstrated that IMERG Final was able to capture large spatial patterns and seasonal and
227 interannual patterns of rainfall. However, fewer studies have explored the performance of the lower
228 latency IMERG Late Runs (DOI: 10.5067/GPM/IMERGDL/DAY/06) product that we use here.
229 Kirshbaum et al. (2016) include a qualitative comparison for CHIRPS Final and IMERG Late for
230 the Southern Africa start-of-season 2015. IMERG Late appears to perform similarly to the 1.5-
231 month latency CHIRPS Final and outperform the 1-day latency NOAA Rainfall Estimate version 2
232 (RFE2) product (Xie and Arkin, 1996). Differences in the daily rainfall distribution patterns
233 between IMERG Final and CHIRPS Final have also been shown to impact the resulting
234 hydrological modeled output in simulations done using the NASA LIS framework (Sarmiento et al.,
235 2021).

236

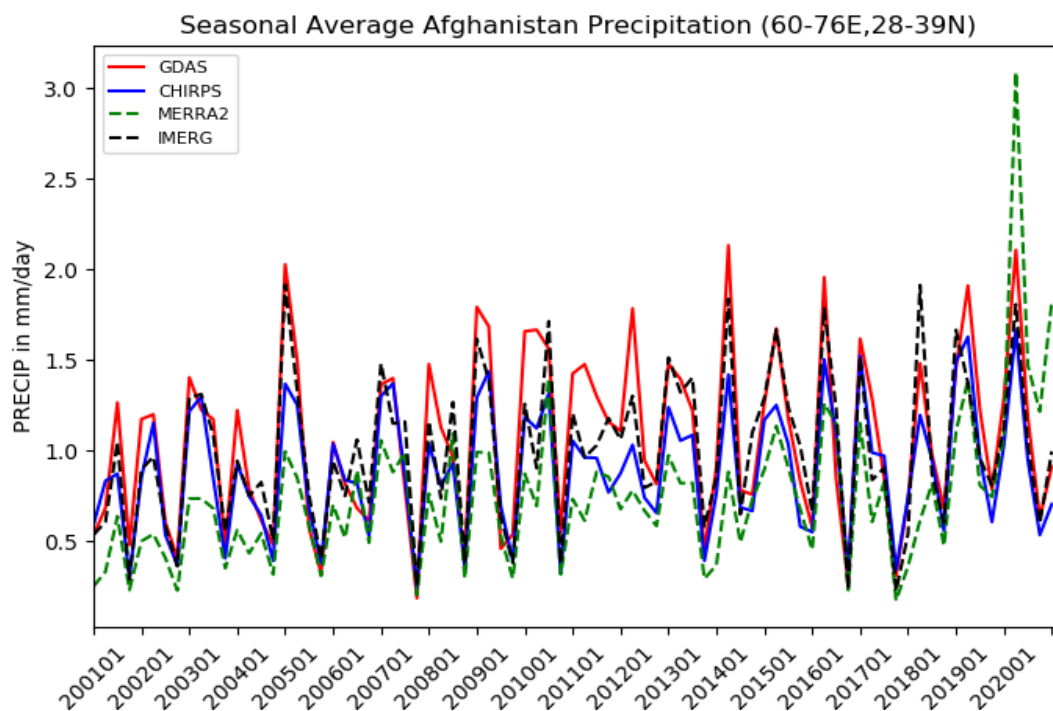


237 For the Snow Cover Fraction (SCF) analysis, we compare the global and Central Asia data streams
238 with the MODIS daily SCF product, MOD10A1 Collection 6 (Hall and Riggs, 2016). MOD10A1
239 data is available at 500 m spatial resolution from February 2000 to the present. SCF is generated
240 using the Normalized Difference Snow Index (NDSI) and additional filters to reduce error and flag
241 uncertainty. Routine qualitative comparisons, which can be viewed on the NASA LIS FEWS NET
242 project website generally show agreement between the model and MODIS SCF, as well as
243 occurrence of cloud cover (<https://ldas.gsfc.nasa.gov/fldas/models/central-asia>). Following
244 Arsenault et al. (2014) we aggregated pixels to 0.01 degree to reduce error related to sensor viewing
245 angles and gridding artifacts. For this analysis, using MODIS SCF as “truth”, we determined True
246 Positives (TP), True Negatives (TN), False Negatives (FN) and False Positives (FP). We then
247 computed probability of detection (POD) where $POD = (TP/(TP + FN))$ and False Alarm Rate
248 (FAR) where $FAR = (FP/(FP + TN))$. We computed these for the total area of Afghanistan, as well
249 as by basin (Fig. 3 a & b). This paper does not compare modeled snow water equivalent (SWE) to
250 independent snow observations because, as noted by Yoon et al. (2019), direct evaluation of snow
251 mass and snow water equivalent (SWE) is difficult over Central Asia due to poor coverage of
252 accurate snow observations. We follow the Yoon et al. (2019) recommendation to conduct
253 quantitative SCF comparisons and provide qualitative SWE analysis in Applications, Section 4.

254 **3 Results**

255 **3.1 Gridded Rainfall Comparison**

256 For Central Asia applications we have two data streams with different precipitation inputs: the
257 global data stream with CHIRPS precipitation at 10 km² spatial resolution provides a long consistent
258 data record, and the Central Asia data stream with GDAS precipitation at 1 km² provides near real
259 time, finer spatial resolution updates. These two data streams have their respective errors and allow
260 data users to apply a convergence of evidence approach for food and water security applications. In
261 this section we present a comparison of these precipitation inputs. We also include IMERG Late for
262 comparison as a high quality, low latency product. Future work will incorporate the IMERG
263 precipitation inputs into FLDAS simulations. We also include MERRA-2 precipitation for
264 comparison. Pair-wise correlation are shown in Table 2. CHIRPS Final, IMERG Late and GDAS (R
265 ≥ 0.90) are well correlated in terms of average daily precipitation (mm/day) at the monthly and
266 annual (i.e., water year) timestep. MERRA-2 correlations with these datasets are lower at the
267 monthly timestep ($0.75 \leq R \leq 0.81$) and annual timestep ($0.64 \leq R \leq 0.69$). Fig. 4 shows the time
268 series of the precipitation products for their overlapping period of record (2001-2020), which
269 illustrates how they co-vary and some general patterns in terms of relative mm/day: GDAS (red) and
270 IMERG Late (dashed-black) tend to have the highest average precipitation per day, CHIRPS (blue)
271 has lower mm/day, but higher than MERRA-2 (dashed green) which tends to have the lowest
272 average precipitation per day, until 2019 when it is notably higher than the other products.



273
274

275 Figure 4. Afghanistan country-wide average, annual average mm/day time series for CHIRPS,
 276 GDAS, IMERG Late, and MERRA-2. At the annual time step, Spearman rank correlations range
 277 from 0.64 (GDAS vs. MERRA-2) to 0.92 (GDAS vs. CHIRPS).
 278

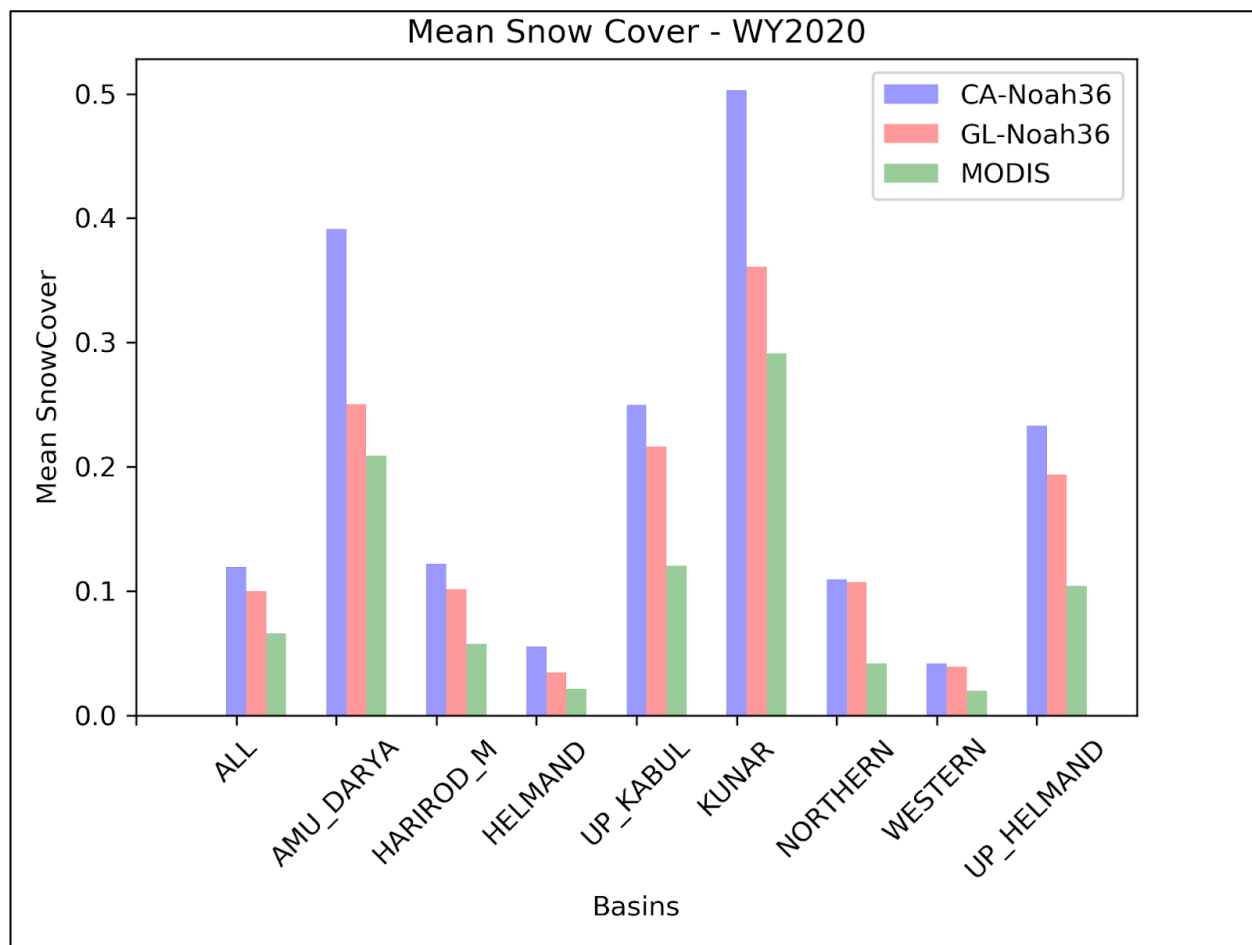
279 Table 2. Afghanistan spatial average Spearman Rank Correlation of monthly (annual) precipitation
 280 2001-2020

	GDAS	CHIRPS Final	IMERG Late
GDAS	x	-	-
CHIRPS Final	0.91 (0.92)	x	-
IMERG Late	0.91 (0.89)	0.92 (0.90)	x
MERRA-2	0.75 (0.64)	0.78 (0.68)	0.81(0.69)

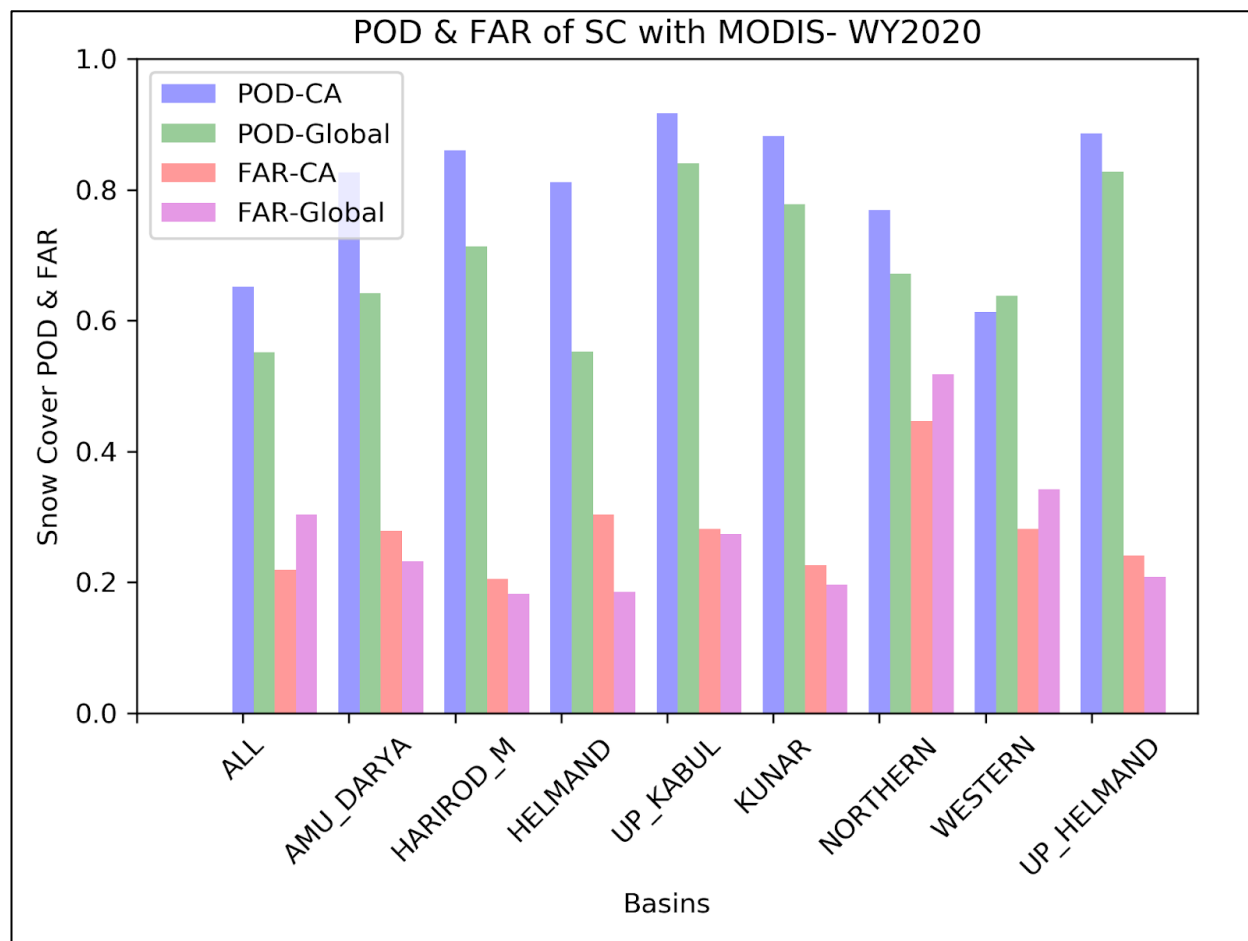
281

282 3.2 Remotely Sensed and Modeled Snow comparisons

283 The estimation of snow is important for Afghanistan and Central Asia because it is an important
 284 contributor to water resources and irrigated agriculture. Here, we compare mean SCF (Fig. 5a),
 285 POD, and FAR statistics (Fig. 5b) relative to MODIS SCF over eight hydrologic basins in
 286 Afghanistan.
 287



288
289 Figure 5a. Mean snow cover fraction for the entire area and by basin for MODIS Snow Cover
290 Fraction (SCF), Central Asia and global data streams.

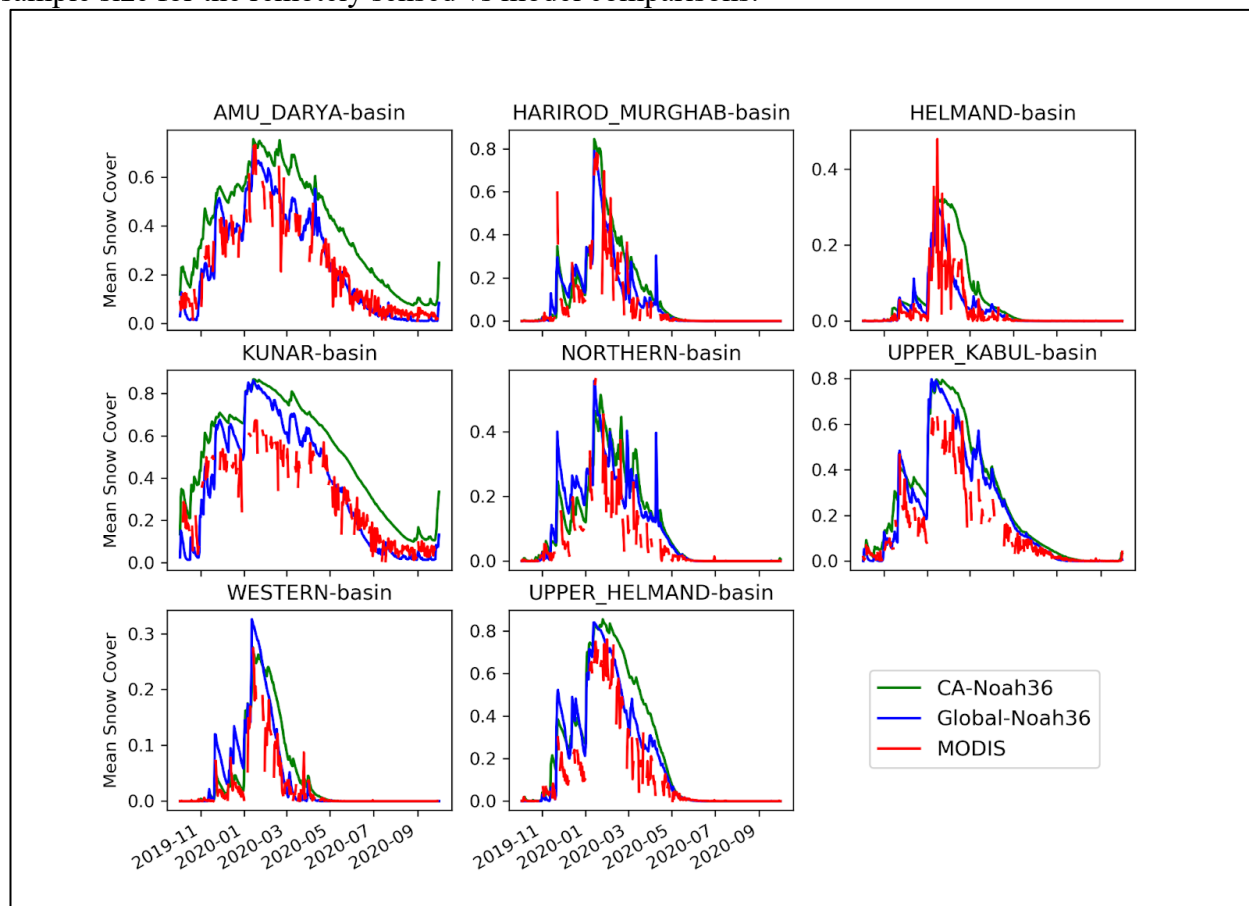


291
292 Figure 5b. Probability of Detection (POD) of snow presence, and False Alarm Rate (FAR) for the
293 Central Asia (CA) and global data streams relative to the MODIS SCF.
294

295 Overall, both model runs estimate greater mean SCF than the MODIS SCF product. The Central
296 Asia (CA) data stream has consistently higher mean snow cover for all basins compared to MODIS
297 SCF estimates and the global data stream. Perhaps not surprisingly then it performs consistently
298 better in POD (by basin = ~80%) except for the Western [Helmand] Basin. Similarly, the FAR of
299 the CA is higher where POD is higher except for the Northern Basin. The difference in statistics
300 may be related to the different inputs forcing or the higher spatial resolution of the Central Asia data
301 stream. Kumar et al. (2013) note that higher spatial resolution was important for snow dominated
302 basins. We also note the likely importance of the MERRA-2 and GDAS temperature forcing
303 between the global data stream and the Central Asia data stream, respectively. The panels in Fig. 6
304 provide additional insight into the differences between MODIS SCF and the two FLDAS runs for
305 water year 2020. The green line (Central Asia) is consistently higher than the red, MODIS SCF
306 estimates, and the blue, global data stream estimates. Both the models estimate higher SCF during
307 peak coverage in the Upper Kabul and Kunar basins. The time series plots also illustrate



308 discontinuities in the MODIS SCF time series, likely related to cloud cover, which reduced the
309 sample size for the remotely sensed vs model comparisons.



310
311 Figure 6. Basin-averaged SCF for Water Year 2020 as estimated by global and Central Asia (CA)
312 data streams, and MODIS SCF. Time series show generally a similar pattern with the CA typically
313 having higher SCF values. These plots also demonstrate discontinuities in the MODIS SCF data that
314 reduce the quality of quantitative comparisons but provide qualitative confirmation of adequate
315 model performance.

316 3.3 Discussion of results compared to previous studies

317 Despite the lack of ground-based observations, our analysis shows that the remotely sensed
318 estimates and the models have good correspondence with other sources of evidence in terms of
319 seasonal timing and performance. This provides analysts with confidence when using the FLDAS
320 snow estimates, in tandem with other sources, as an input to food security analysis. Our approach is
321 supported by other studies that have explored the challenges of evaluating hydrologic estimates over
322 the region (Yoon et al., 2019; Ghatak et al., 2018; Immerzeel et al., 2015; Qamer et al., 2019). With
323 a study domain shifted to the east, Yoon et al. (2019) evaluate rainfall and near surface temperature
324 estimates over the High Mountain Asia domain, including most of Afghanistan. They review how



325 these results compare to other studies (e.g. precipitation trends (Nguyen et al., 2018; Rodell et al.,
 326 2018)), and their results suggest that the uncertainty in the meteorologic forcing is the dominant
 327 factor in the terrestrial water budget estimates. This is consistent with our results showing
 328 differences between the GDAS and CHIRPS+MERRA-2 driven outputs. Also consistent with our
 329 results, Yoon et al. (2019) show that their LSM ensembles of SCF have an average POD of 72% and
 330 FAR of 36%, which is within the range of our POD and FAR statistics (60-80% POD; 20-40%
 331 FAR) compared to MODIS SCF. Without a clear “winner” in their multi-model and multi-forcing
 332 experiments, Yoon et al. conclude that improvements in the meteorological boundary conditions
 333 would be needed to reduce the uncertainty in the terrestrial budget estimates. These sentiments are
 334 echoed in Qamer et al. (2019).

335
 336 One recent attempt to improve meteorological inputs in the region is from Ma et al. (2020) with the
 337 development of the AIMERG dataset that combines IMERG Final with APHRODITE (Asian
 338 Precipitation - Highly-Resolved Observational Data Integration Toward Evaluation) rain-gauge
 339 derived product (Yatagai et al., 2012). Ultimately, it would be beneficial to have a global modeling
 340 system that used the best available inputs from each region. In the meantime, multi-forcing and
 341 multi-model ensembles, and convergence of evidence with other remotely sensed data and field
 342 reports, are a viable approach for providing hydrologic estimates for various applications.

343 3.4 Summary of differences between the model runs

344 Given the need for multiple data streams for convergence of evidence, we have summarized the pros
 345 and cons of the Central Asia and global data streams in Table 3.

346
 347 Table 3. Pros and cons of the two data streams

	Central Asia: Noah 3.6 with GDAS (2000-present)	Global: Noah 3.6 with CHIRPS+MERRA-2 (1982-present)
PROS	1 km ²	less computationally intensive
	1 day latency, daily timestep	longer time record
	Snow estimates available in USGS Early Warning eXplorer	CHIRPS & MERRA-2 forcing spatial resolution does not change over time (stable climatology)
		Water and Energy balance available in NASA GIOVANNI, Google Earth Engine, Climate Engine
CONS	more computationally intensive	lower resolution (10 km ²)



	shorter time record	~30-day latency
	GDAS forcing resolution changes over time (unstable climatology) NOAA NCEP https://www.emc.ncep.noaa.gov/gmb/STATS/html/model_changes.html)	not publicly available at daily timestep
	large data volume, difficult to move	

348 4 Applications

349 These data from global and Central Asia data streams are routinely used in several FEWS NET
 350 information products listed in Table 4. There is a weekly briefing from NOAA’s Climate Prediction
 351 Center (CPC) International Desks on the past week’s weather conditions and 1– 2-week forecasts
 352 for FEW NET regions of interest, including Central Asia. There is also a monthly FEWS NET
 353 Seasonal Monitor and a monthly Seasonal Forecast Review for which these data provide
 354 information on the current state of the snowpack, soil moisture and runoff. These “observed
 355 conditions” can then be qualitatively combined with forecasts ranging from 1 week to 3 months to
 356 assess potential hydro-meteorological hazards. To demonstrate the role of these data in the early
 357 warning process, at different points in the season, we provide an example of the 2017-2018 wet
 358 season in Afghanistan during a La Niña event.

359
 360 Table 4. Routine Applications of FLDAS Central Asia’s Afghanistan hydrologic data.

Routine application of these data	Weblink to updates	Notes
FEWS NET Global Weather Hazards Summary produced by NOAA CPC	https://fews.net/global/global-weather-hazards/ https://www.cpc.ncep.noaa.gov/products/international/index.shtml	shapefiles https://ftp.cpc.ncep.noaa.gov/fews/weather_hazards/
USGS Seasonal Monitor	https://earlywarning.usgs.gov/fews/search/Asia/Central%20Asia/Afghanistan Archives: https://fews.net/sectors-topics/sectors/agroclimatology	Updated monthly from October - May, during the precipitation season.

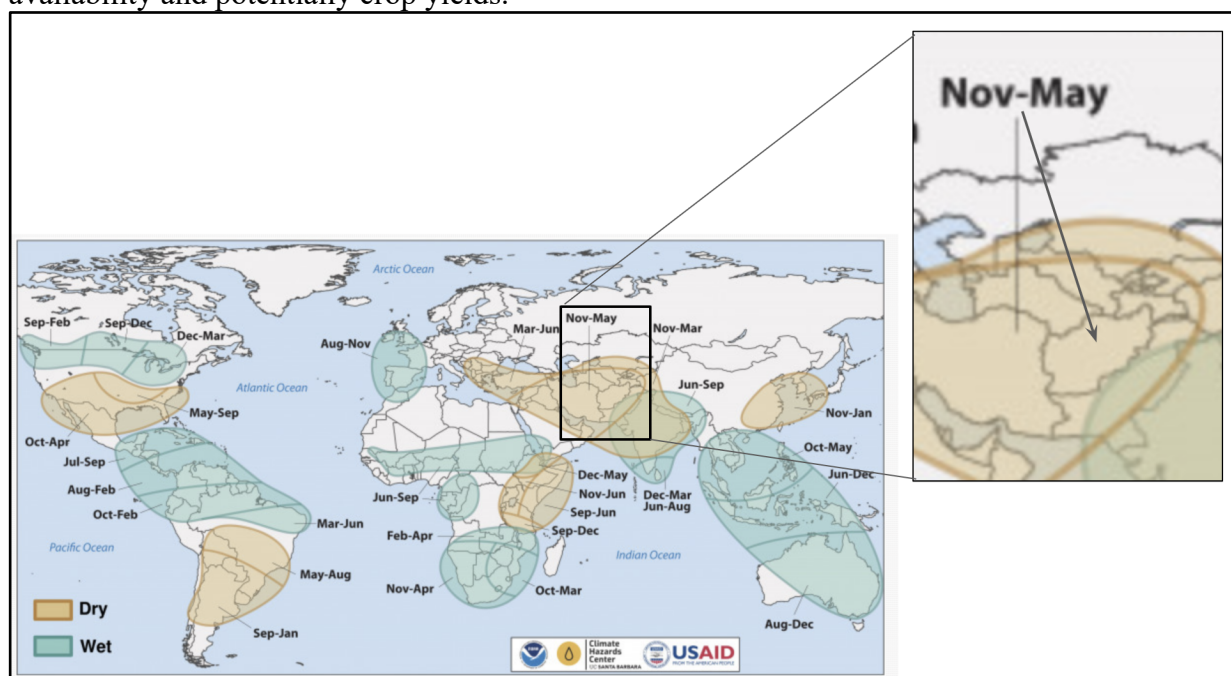


FEWS NET Food Security Outlook Brief	https://fews.net/central-asia/afghanistan	Information on snow or other hydrology included if applicable
Crop Monitor for Early Warning	https://cropmonitor.org/index.php/cmreports/early-warning-report/	Information on early warning and crop conditions

361

362 **4.1 Snow monitoring & Seasonal Outlooks**

363 As previously mentioned, and as shown in Fig. 7, Afghanistan and the broader region is strongly
 364 influenced by La Niña, which tends to increase the likelihood of dry events (Barlow et al., 2016;
 365 FEWS NET, 2020b). Depending on other factors, this may also increase the probability of negative
 366 snowpack anomalies, reduce springtime streamflow, and flood risk, and reduce summer irrigation
 367 availability and potentially crop yields.



368 Figure 7. Timing of wet and dry conditions related to La Niña. Increased likelihood of dry
 369 conditions from Nov-May for Afghanistan during La Niña events.
 370

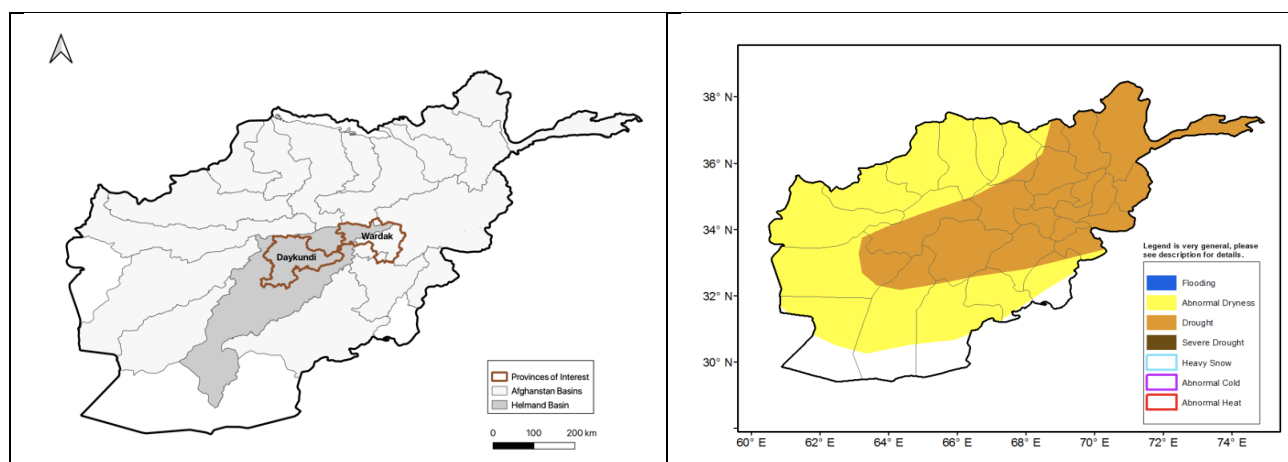
371
 372 A La Niña Watch was issued by NOAA in September 2017 (NOAA, 2017). The FEWS NET
 373 October 2017 Food Security Outlook (FEWS NET, 2017a) stated that La Niña conditions were
 374 expected throughout the northern hemisphere fall and winter and that below-average precipitation
 375 was likely over much of Central Asia, including Afghanistan, during the 2017-2018 wet season.
 376 With the expectation of below average rainfall coupled with above average temperature forecasts,
 377 FEWS NET anticipated that snowpack would most likely be below average. In the context of food



378 security outcomes, it was assumed that areas planted with winter wheat were likely to be lower than
379 usual, reducing land preparation activities and associated demand for labor. Two provinces of
380 particular concern were Daykundi and Wardak (Fig. 8a brown borders), both located in the
381 Helmand River Basin (Fig. 8a; grey shading). Precipitation deficits in these provinces would lead to
382 poor rangeland resources and pasture availability and would likely result in decreased livestock
383 productivity and milk production through May. However, given that October was the very start of
384 the wet season, there remained a large spread of possible outcomes: spatial and temporal rainfall
385 distributions, and snowpack totals necessitating routine updates to assumptions.

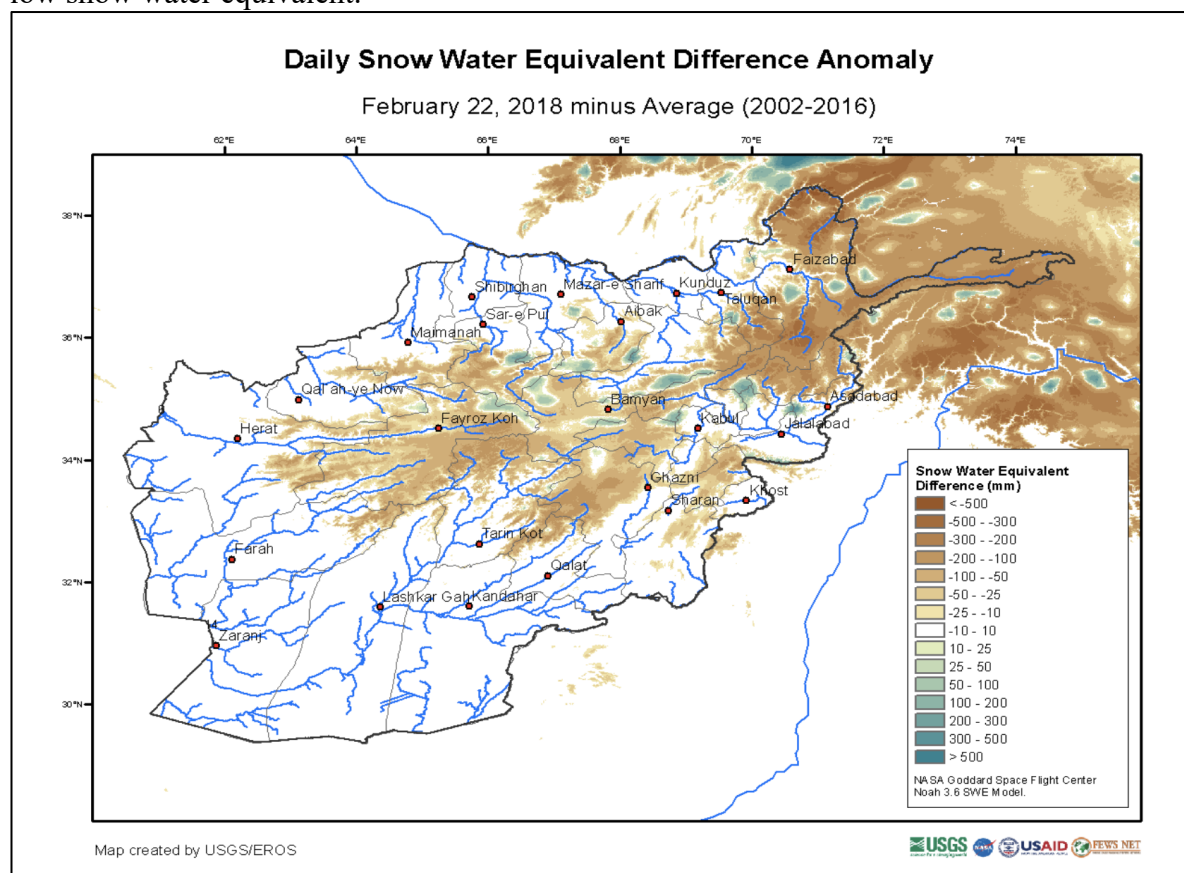
387 Monitoring continued onward in the season from October, tracking observations from remote
388 sensing, models, and field reports as well as weather, sub-seasonal and seasonal forecasts. This
389 information was used to regularly update expectations of end of season outcomes. Using the FLDAS
390 Central Asia data stream, a December 21, 2017, NOAA CPC Weather Hazards Brief reported that
391 parts of northern and central Afghanistan remained atypically snow free, and north-eastern high
392 elevation areas exhibited snow water equivalent (SWE) deficits. SWE is a commonly used
393 measurement of the amount of liquid water contained within the snowpack, and an indicator of the
394 amount of water that will be released from the snowpack when it melts. By January 17, 2018, an
395 abnormal dryness polygon was placed over northeast Afghanistan, the central highlands of
396 Afghanistan based on below average snow water equivalent values from the FLDAS Central Asia
397 estimates. Abnormal dryness is defined for an area that has registered cumulative 4-week
398 precipitation and soil moisture ranking less than the 30th percentile, with a Standardized
399 Precipitation Index (SPI) of 0.4 standard deviation below the mean. In addition, it is required that
400 forecasts indicate below-average precipitation (less than 80% of normal) for that area during the 1-
401 week outlook period. By late February 2018, precipitation deficits and related SWE (Fig. 9)
402 increased and met the criteria for “drought” (Fig. 8b). Drought is defined as an area that has
403 previously been defined as “Abnormal Dryness” and has continued to register seasonal precipitation
404 and soil moisture deficits since the beginning of the rainfall season. Specifically, an eight-week
405 cumulative precipitation, soil moisture, and runoff below the 20th percentile rank, and an SPI of 0.8
406 standard deviation below the mean are classification guidelines.

407





408
409 Figure 8. (a) Map showing hydrological basins, with Helmand Basin in darker grey and location of
410 Daykundi and Wardak provinces where food security conditions were of particular concern (b)
411 NOAA CPC Afghanistan Hazard Report February 22-28, 2018 (CPC NOAA, 2018), map showing
412 widespread abnormal dryness and drought, defined by 90-day precipitation deficits and extremely
413 low snow water equivalent.



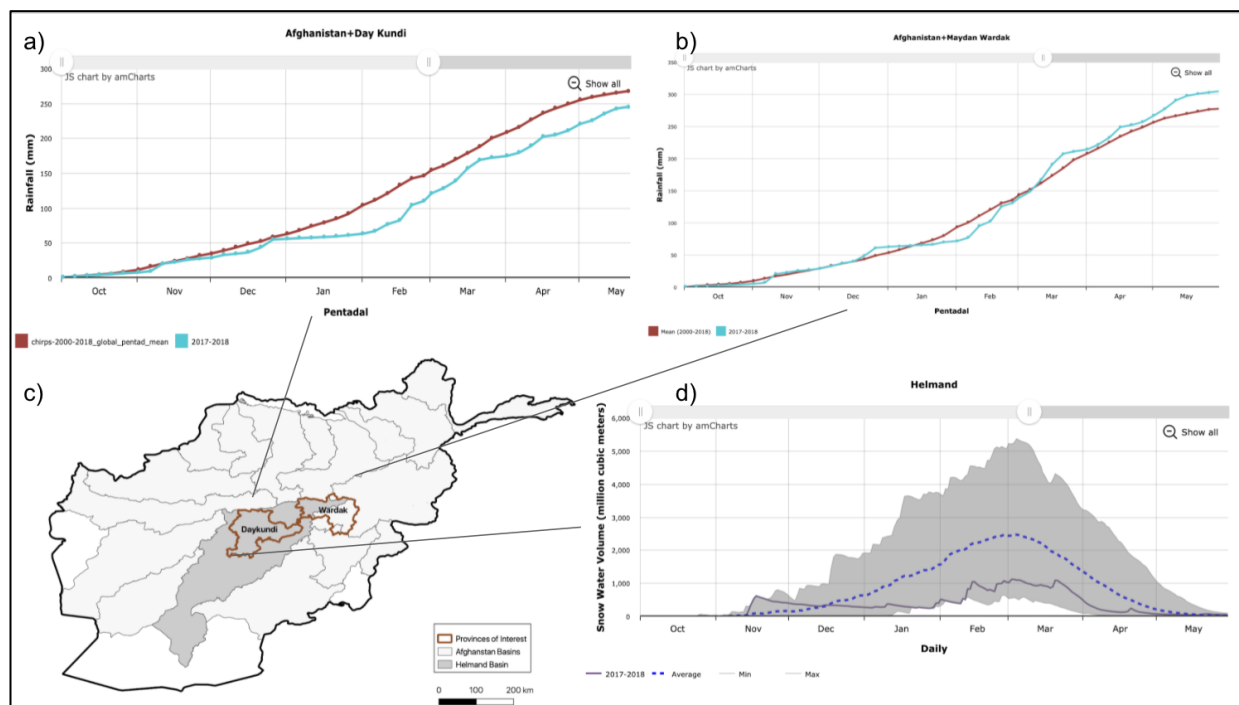
414
415 Figure 9. FLDAS Central Asia snow water equivalent (SWE) estimates for February 22, 2018.
416 SWE deficits of >300 mm were widespread at this time.

417
418 The February 2018 Food Security Outlook (FEWS NET, 2018b) provided the following updates,
419 based on the CPC Hazards Reports and Seasonal Monitors: “Snow accumulation and cumulative
420 precipitation were well below average for the season through February 2018, with some basins at or
421 near record low snowpack, with data since 2002....These factors will likely have an adverse impact
422 on staple production in marginal irrigated areas and in many rainfed areas. [Moreover, with]
423 forecasts for above-average temperatures during the spring and summer, rangeland conditions are
424 expected to be poor during the period of analysis through September 2018. This could have an
425 adverse impact on pastoralists and agro-pastoralists, particularly in areas where livestock
426 movements are limited by conflict.” The Crop Monitor for Early Warning February and March 2018



427 reports (GEOGLAM, 2018a, b) also cited reduced snowpack in Afghanistan and the negative
428 impacts on winter wheat crops as well as irrigation water availability in the Spring. The story was
429 also highlighted in NASA Earth Observatory March 2018 “Record Low Snowpack in Afghanistan”
430 (Record Low Snowpack in Afghanistan, 2018).

431
432 The USGS’s Early Warning eXplorer (Shukla et al., 2021) allows analysts to look at maps and time
433 series for a variety of variables and specific provinces and river basins. Plots from EWX in Fig. 10
434 show below average precipitation in provinces in the Helmand Basin for January and February.
435 CHIRPS cumulative rainfall for 2017-18 vs the 18-year average for Day Kundi (a.k.a. Daykundi)
436 Province showed near average conditions until December. From January cumulative rainfall
437 remained below the 2000-2018 average throughout the rest of the season ending in May; the same
438 pattern occurred in nearby Uruzgan Province. In neighboring Maydan Wardak (a.k.a Wardak)
439 Province below average conditions were experienced in January and February but recovered in
440 March to remain slightly above average. Day Kundi (Fig. 10a) and Wardak (Fig. 10b) are provinces
441 located in the upper reaches of the Helmand Basin. Fig. 10d shows SWE averaged across the entire
442 Helmand basin. The grey shading indicates the range of the minimum and maximum values, and the
443 dashed blue line is the average. Initial snow conditions start above average until December when
444 SWE deficits are near record low values through the beginning of February, and then persist at
445 below-average levels.
446



447
448 Figure 10. CHIRPS cumulative rainfall for 2017-18 vs average conditions for (a) Daykundi
449 Province (b) Maydan Wardak Province. (c) Map showing location of Daykundi and Wardak
450 provinces, and the Helmand Basin where food security conditions were of particular concern. (d)



451 Helmand Basin snow water equivalent (SWE) from the Central Asia data stream. The grey shading
452 indicates the range of the minimum and maximum values, dashed blue line is the average, and black
453 line is 2017-18.

454
455 By the end of season in April 2018, FEWS NET (2018c) concluded that “below-average
456 precipitation throughout most of the country during the October 2017 – May 2018 wet season has
457 led to very low snowpack ...Low irrigation water availability is likely to have an adverse impact on
458 yields for winter wheat and other ...barley, maize, and others.. particularly in downstream areas in
459 regions with limited rainfall. ...The poor performance of the wet season and above average
460 temperatures... exacerbated dry rangeland conditions in many areas, particularly in ..Sari Pul, [and
461 surrounding] ...provinces. Pastoralists and agropastoralists in these areas will likely attempt to
462 migrate to areas with better pasture and water availability or sell livestock at below-average prices.”
463 At the same time UNICEF reported in April 2018 (500,000 children affected by drought in
464 Afghanistan – UNICEF, 2018) that among “the [drought] affected provinces, Baghis, Bamyan,
465 Daykundi, Ghor, Helmand, ... and Uruzgan are of critical priority for nutrition and water, sanitation
466 and hygiene assistance”.

467
468 Several months after a season and harvest has ended more statistics become available for further
469 verification of the drought outcomes. The FEWS NET October 2018 Food Security Outlook (2018a)
470 reported that the 2017/18 drought had significant negative impacts on rainfed wheat production and
471 livestock pasture and body conditions across the country. Reporting statistics from the Afghanistan
472 Ministry of Agriculture, Irrigation, and Livestock, the total wheat production for the 2017/18
473 agriculture season was about 20% below average, where irrigated agriculture performed about
474 average. However, rainfed agriculture production was only about 50% of average, most severely
475 impacting households in in Badakhshan, Badhis, and Daykundi provinces where dry conditions,
476 insecurity, poor incomes, and depleted assets were expected to continue to face emergency food
477 insecurity though May 2019 characterized by large food consumption gaps reflected in acute
478 malnutrition or are employing emergency coping strategies.

479 **5. Data Availability**

480 The Central Asia data described in this manuscript can be accessed at the NASA GES DISC
481 repository under data doi 10.5067/VQ4CD3Y9YC0R. The data citation is the following:

482
483 Jacob, Jossy and Slinski, Kimberly (NASA/GSFC/HSL) (2021), FLDAS Noah Land Surface Model
484 L4 Central Asia Daily 0.01 x 0.01 degree, Greenbelt, MD, USA, Goddard Earth Sciences Data and
485 Information Services Center (GES DISC), Accessed: [*Data Access Date*],
486 [10.5067/VQ4CD3Y9YC0R](https://doi.org/10.5067/VQ4CD3Y9YC0R)

487
488 The Global data described in this manuscript can be accessed at the NASA GES DISC repository
489 under data doi 10.5067/5NHC22T9375G. The data citation is the following:



490
491 McNally, Amy. NASA/GSFC/HSL (2018), FLDAS Noah Land Surface Model L4 Global Monthly
492 0.1 x 0.1 degree (MERRA-2 and CHIRPS), Greenbelt, MD, USA, Goddard Earth Sciences Data and
493 Information Services Center (GES DISC), Accessed: [Data Access Date], 10.5067/5NHC22T9375G
494
495 Currently the USGS EROS Center provides images from these data:
496 <https://earlywarning.usgs.gov/fews/search/Asia/Central%20Asia>, as well as an interactive data
497 viewer, the USGS Early Warning eXplorer (EWX) [https://earlywarning.usgs.gov/fews/software-](https://earlywarning.usgs.gov/fews/software-tools/1)
498 [tools/1](https://earlywarning.usgs.gov/fews/software-tools/1) (Shukla et al. 2021).

499 6. Code availability

500 The NASA Land Information System Framework (LISF) is publicly available and an open-source
501 software. The software and technical support are available at <https://github.com/NASA-LIS/LISF>.

502 7. Conclusion

503 This paper describes a comprehensive hydrologic analysis system for food security monitoring in
504 Central Asia, with analysis focusing on Afghanistan. Our intent is to provide the reader with
505 substantial information regarding the configuration and specification of both the current global and
506 Central Asia data streams. These data are publicly available and available at near-real time for food
507 security decision support. An important note is that, as an on-going initiative, FLDAS model version
508 and parameters are routinely updated, and the user should consult the version updates provided by
509 the NASA GES DISC data provider and documentation on USGS Early Warning website. For
510 example, efforts are currently underway to upgrade to the Noah with multi parameterizations (Noah-
511 MP) (Niu et al., 2011) land surface model, which requires some changes in parameters for snow,
512 glaciers and groundwater. This, and future changes will be informed by the strengths and
513 weaknesses of the data stream configurations that we have discussed in this paper.

514
515 This paper also provides model-model and model-remote sensing comparisons, as well as a review
516 of other research that highlights the challenges of quantitative evaluation of models and remote
517 sensing in this region. A key challenge to hydrologic modeling is the considerable uncertainty in the
518 meteorological forcing, particularly precipitation, available for this region. Advancements in remote
519 sensing and modeling should help reduce these uncertainties. In addition, the current land surface
520 modeling and river routing frameworks reflect natural conditions, i.e., they do not include
521 representation of anthropogenic impacts such as human water abstractions (e.g., dams for flood
522 control or irrigation, water diversions, groundwater pumping, etc.) or land application of abstracted
523 water (i.e., irrigation). These factors impact streamflow (through abstraction and irrigation flows) as
524 well as estimates of soil moisture, evapotranspiration, and sensible heat flux (land surface
525 temperatures) in irrigated areas. Therefore, it is important to be aware of the limitations and
526 combine with other products (e.g., Normalized Difference Vegetation Index (NDVI) or Actual



527 Evapotranspiration (ETa) in irrigated areas) when exploring water and energy balance. Even with
528 improvements to meteorological forcing and modeling parameterizations, errors will remain.
529 Therefore, the ‘convergence of evidence’ approach that we advocate for here will continue to be
530 important when assessing hydro-meteorological hazards and associated risks to food and water
531 security. We hope that by making the data publicly available the broader food security and water
532 resources communities will be able to provide insights that will lead to improvements in our
533 understanding of the water and energy balance that will ultimately lead to improvements to food and
534 water security decision support systems.

535

536 **8. Author contribution**

537 JJ runs the code, updates websites and archives routinely. DS maintains LIS code used in paper, JJ,
538 KA, DS, SP conducted model evaluation AM, KS, CPL, SK contributed to design of evaluation. JR,
539 MB, SP manage the data for USGS distribution. AH, JV provides feedback on data quality and
540 interpretation. AM prepared the manuscript with contributions from all co-authors.

541 **9. Acknowledgements**

542 The authors wish to acknowledge the original version of the Central Asia snow modeling with LIS6
543 performed at NOAA National Operational Hydrologic Remote Sensing Center by Greg Fall and
544 Logan Karsten. USGS work was performed under USGS contract 140G0119C0001. Any use of
545 trade, firm, or product names is for descriptive purposes only and does not imply endorsement by
546 the U.S. Government. KS, AH, DS, JJ, NASA work was performed under U.S. Agency for
547 International Development, Bureau of Humanitarian Assistance PAPA AID-FFP-T-17-00001. KS,
548 AH acknowledge support from the NASA Harvest Consortium (NASA Applied Sciences Grant No.
549 80NSSC17K0625). Computing resources have been provided by NASA’s Center for Climate
550 Simulation (NCCS). Distribution of data from the Goddard Earth Sciences Data and Information
551 Services Center (GES DISC) is funded by NASA's Science Mission Directorate (SMD). We thank
552 NOAA CPC International Desk for use of Figures. The NASA Land Information System Team for
553 software support and development. The authors also thank the USGS reviewer for comments that
554 improved the quality of the manuscript.

555 **10. References**

556 Arsenault, K. R., Houser, P. R., and De Lannoy, G. J. M.: Evaluation of the MODIS snow cover
557 fraction product: Satellite-based snow cover fraction evaluation., *Hydrol. Process.*, 28, 980–998,
558 <https://doi.org/10.1002/hyp.9636>, 2014.

559 Arsenault, K. R., Kumar, S. V., Geiger, J. V., Wang, S., Kemp, E., Mocko, D. M., Beaudoin, H.
560 K., Getirana, A., Navari, M., Li, B., Jacob, J., Wegiel, J., and Peters-Lidard, C. D.: The Land surface
561 Data Toolkit (LDT v7.2) – a data fusion environment for land data assimilation systems, 11, 3605–
562 3621, <https://doi.org/10.5194/gmd-11-3605-2018>, 2018.



- 563 Barlow, M., Wheeler, M., Lyon, B., and Cullen, H.: Modulation of Daily Precipitation over
564 Southwest Asia by the Madden–Julian Oscillation, 133, 3579–3594,
565 <https://doi.org/10.1175/MWR3026.1>, 2005.
- 566 Barlow, M., Zaitchik, B., Paz, S., Black, E., Evans, J., and Hoell, A.: A Review of Drought in the
567 Middle East and Southwest Asia, 29, 8547–8574, <https://doi.org/10.1175/JCLI-D-13-00692.1>, 2016.
- 568 Carroll, M., DiMiceli, C., Wooten, M., Hubbard, A., Sohlberg, R., and Townshend, J.: MOD44W
569 MODIS/Terra Land Water Mask Derived from MODIS and SRTM L3 Global 250m SIN Grid V006
570 [Data set]. NASA EOSDIS Land Processes DAAC., NASA EOSDIS Land Processes DAAC.,
571 NASA EOSDIS Land Processes DAAC., 2017.
- 572 Chen, F., Mitchell, K., Schaake, J., Xue, Y., Pan, H.-L., Koren, V., Duan, Q. Y., Ek, M., and Betts,
573 A.: Modeling of land surface evaporation by four schemes and comparison with FIFE observations,
574 *J. Geophys. Res.*, 101, 7251–7268, <https://doi.org/10.1029/95JD02165>, 1996.
- 575 CIA World Factbook: <https://www.cia.gov/the-world-factbook/countries/afghanistan/#introduction>.
- 576 Cosgrove, B. A., Lohmann, D., Mitchell, K. E., Houser, P. R., Wood, E. F., Schaake, J. C., Robock,
577 A., Marshall, C., Sheffield, J., Duan, Q., Luo, L., Higgins, R. W., Pinker, R. T., Tarpley, J. D., and
578 Meng, J.: Real-time and retrospective forcing in the North American Land Data Assimilation
579 System (NLDAS) project, *J. Geophys. Res.*, 108, 2002JD003118,
580 <https://doi.org/10.1029/2002JD003118>, 2003.
- 581 CPC NOAA: Weather Hazards Outlook of Afghanistan and Central Asia for the Period of February
582 22 - 28, 2018, 2018.
- 583 Davenport, F. M., Harrison, L., Shukla, S., Husak, G., Funk, C., and McNally, A.: Using out-of-
584 sample yield forecast experiments to evaluate which earth observation products best indicate end of
585 season maize yields, *Environ. Res. Lett.*, 14, 124095, <https://doi.org/10.1088/1748-9326/ab5ccd>,
586 2019.
- 587 Derber, J. C., Parrish, D. F., and Lord, S. J.: The New Global Operational Analysis System at the
588 National Meteorological Center, 6, 538–547, [https://doi.org/10.1175/1520-0434\(1991\)006<0538:TNGOAS>2.0.CO;2](https://doi.org/10.1175/1520-0434(1991)006<0538:TNGOAS>2.0.CO;2), 1991.
- 590 Dezfuli, A. K., Ichoku, C. M., Huffman, G. J., Mohr, K. I., Selker, J. S., van de Giesen, N.,
591 Hochreutener, R., and Annor, F. O.: Validation of IMERG Precipitation in Africa, 18, 2817–2825,
592 <https://doi.org/10.1175/JHM-D-17-0139.1>, 2017.
- 593 Ek, M. B., Mitchell, K. E., Lin, Y., Rogers, E., Grunmann, P., Koren, V., Gayno, G., and Tarpley, J.
594 D.: Implementation of Noah land surface model advances in the National Centers for Environmental
595 Prediction operational mesoscale Eta model, 108, <https://doi.org/10.1029/2002JD003296>, 2003.



- 596 Fall, G.: NOAA National Operational Hydrologic Remote Sensing Center, 2014.
- 597 FEWS NET: Afghanistan Food Security Outlook October 2017-May 2018 Conflict, dry spells, and
598 weak labor opportunities will lead to deterioration in outcomes during 2018 lean season, 2017a.
- 599 FEWS NET: Update on performance of the October 2016 – May 2017 wet season, 2017b.
- 600 FEWS NET: Afghanistan Food Security Outlook: Emergency assistance needs are atypically high
601 through the lean season across the country, FEWS NET, 2018a.
- 602 FEWS NET: Afghanistan Food Security Outlook February to September 2018: Low snow
603 accumulation and dry soil conditions likely to impact 2018 staple production, 2018b.
- 604 FEWS NET: Afghanistan Food Security Outlook Update April 2018: Poor rangeland conditions and
605 below-average water availability will limit seasonal improvements, 2018c.
- 606 FEWS NET: El Niño and Precipitation, FEWS NET, <https://fews.net/el-ni%C3%B1o-and-precipitation>, 2020a.
- 607
- 608 FEWS NET: La Niña and Precipitation, FEWS NET, <https://fews.net/la-ni%C3%B1a-and-precipitation>, 2020b.
- 609
- 610 FEWS NET: Afghanistan Food Security Outlook February to September 2021: Below-average
611 precipitation likely to drive below-average agricultural and livestock production in 2021, 2021.
- 612 Funk, C., Peterson, P., Landsfeld, M., Pedreros, D., Verdin, J., Shukla, S., Husak, G., Rowland, J.,
613 Harrison, L., Hoell, A., and Michaelsen, J.: The climate hazards infrared precipitation with stations--
614 a new environmental record for monitoring extremes., The climate hazards infrared precipitation
615 with stations—a new environmental record for monitoring extremes, *Sci Data*, 2, 2, 150066–
616 150066, <https://doi.org/10.1038/sdata.2015.66>, 10.1038/sdata.2015.66, 2015.
- 617 Gadelha, A. N., Coelho, V. H. R., Xavier, A. C., Barbosa, L. R., Melo, D. C. D., Xuan, Y.,
618 Huffman, G. J., Petersen, W. A., and Almeida, C. das N.: Grid box-level evaluation of IMERG over
619 Brazil at various space and time scales, *Atmospheric Research*, 218, 231–244,
620 <https://doi.org/10.1016/j.atmosres.2018.12.001>, 2019.
- 621 Gelaro, R., McCarty, W., Suárez, M. J., Todling, R., Molod, A., Takacs, L., Randles, C. A.,
622 Darmenov, A., Bosilovich, M. G., Reichle, R., Wargan, K., Coy, L., Cullather, R., Draper, C.,
623 Akella, S., Buchard, V., Conaty, A., da Silva, A. M., Gu, W., Kim, G.-K., Koster, R., Lucchesi, R.,
624 Merkova, D., Nielsen, J. E., Partyka, G., Pawson, S., Putman, W., Rienecker, M., Schubert, S. D.,
625 Sienkiewicz, M., and Zhao, B.: The Modern-Era Retrospective Analysis for Research and
626 Applications, Version 2 (MERRA-2), *J. Climate*, 30, 5419–5454, <https://doi.org/10.1175/JCLI-D-16-0758.1>, 2017.
- 627



- 628 GEOGLAM: Early Warning Crop Monitor February 2018,
629 https://cropmonitor.org/documents/EWCM/reports/EarlyWarning_CropMonitor_201802.pdf,
630 2018a.
- 631 GEOGLAM: Early Warning Crop Monitor March 2018,
632 https://cropmonitor.org/documents/EWCM/reports/EarlyWarning_CropMonitor_201802.pdf,
633 2018b.
- 634 Ghatak, D., Zaitchik, B., Kumar, S., Matin, M. A., Bajracharya, B., Hain, C., and Anderson, M.:
635 Influence of Precipitation Forcing Uncertainty on Hydrological Simulations with the NASA South
636 Asia Land Data Assimilation System, 5, 57, <https://doi.org/10.3390/hydrology5040057>, 2018.
- 637 Grace, K. and Davenport, F.: Climate variability and health in extremely vulnerable communities:
638 investigating variations in surface water conditions and food security in the West African Sahel,
639 *Population & Environment*, 42, 553–577, <https://doi.org/10.1007/s11111-021-00375-9>, 2021.
- 640 Hall, D. and Riggs, G.: MODIS/Terra Snow Cover Daily L3 Global 500m SIN Grid,
641 <https://doi.org/10.5067/MODIS/MOD10A1.006>, 2016.
- 642 Hoell, A., Funk, C., and Barlow, M.: The Forcing of Southwestern Asia Teleconnections by Low-
643 Frequency Sea Surface Temperature Variability during Boreal Winter, 28, 1511–1526,
644 <https://doi.org/10.1175/JCLI-D-14-00344.1>, 2015.
- 645 Hoell, A., Barlow, M., Cannon, F., and Xu, T.: Oceanic Origins of Historical Southwest Asia
646 Precipitation During the Boreal Cold Season, *J. Climate*, 30, 2885–2903,
647 <https://doi.org/10.1175/JCLI-D-16-0519.1>, 2017.
- 648 Hoell, A., Cannon, F., and Barlow, M.: Middle East and Southwest Asia Daily Precipitation
649 Characteristics Associated with the Madden–Julian Oscillation during Boreal Winter, *J. Climate*, 31,
650 8843–8860, <https://doi.org/10.1175/JCLI-D-18-0059.1>, 2018.
- 651 Hoell, A., Eischeid, J., Barlow, M., and McNally, A.: Characteristics, precursors, and potential
652 predictability of Amu Darya Drought in an Earth system model large ensemble, *Clim Dyn*, 55,
653 2185–2206, <https://doi.org/10.1007/s00382-020-05381-5>, 2020.
- 654 Huffman, G. J., Bolvin, D. T., Braithwaite, D., Hsu, K.-L., Joyce, R. J., Kidd, C., Nelkin, E. J.,
655 Sorooshian, S., Stocker, E. F., Tan, J., Wolff, D. B., and Xie, P.: Integrated Multi-satellite Retrievals
656 for the Global Precipitation Measurement (GPM) Mission (IMERG), in: *Satellite Precipitation
657 Measurement: Volume 1*, edited by: Levizzani, V., Kidd, C., Kirschbaum, D. B., Kummerow, C. D.,
658 Nakamura, K., and Turk, F. J., Springer International Publishing, Cham, 343–353,
659 https://doi.org/10.1007/978-3-030-24568-9_19, 2020.



- 660 Immerzeel, W. W., Wanders, N., Lutz, A. F., Shea, J. M., and Bierkens, M. F. P.: Reconciling high-
661 altitude precipitation in the upper Indus basin with glacier mass balances and runoff, 19, 4673–4687,
662 <https://doi.org/10.5194/hess-19-4673-2015>, 2015.
- 663 Jacob, J. and Slinski, K.: GES DISC Dataset: FLDAS Noah Land Surface Model L4 Central Asia
664 Daily 0.01 x 0.01 degree (FLDAS_NOAH001_G_CA_D 001), 2021.
- 665 Jung, H. C., Getirana, A., Policelli, F., McNally, A., Arsenault, K. R., Kumar, S., Tadesse, T., and
666 Peters-Lidard, C. D.: Upper Blue Nile basin water budget from a multi-model perspective, *Journal*
667 *of Hydrology*, 555, 535–546, <https://doi.org/10.1016/j.jhydrol.2017.10.040>, 2017.
- 668 Jung, H. C., Getirana, A., Arsenault, K. R., Holmes, T. R. H., and McNally, A.: Uncertainties in
669 Evapotranspiration Estimates over West Africa, 11, 892, <https://doi.org/10.3390/rs11080892>, 2019.
- 670 Kirschbaum, D. B., Huffman, G. J., Adler, R. F., Braun, S., Garrett, K., Jones, E., McNally, A.,
671 Skofronick-Jackson, G., Stocker, E., Wu, H., and Zaitchik, B. F.: NASA’s Remotely Sensed
672 Precipitation: A Reservoir for Applications Users, *Bull. Amer. Meteor. Soc.*, 98, 1169–1184,
673 <https://doi.org/10.1175/BAMS-D-15-00296.1>, 2016.
- 674 Kumar, S. V., Peters-Lidard, C. D., Tian, Y., Houser, P. R., Geiger, J., Olden, S., Lighty, L.,
675 Eastman, J. L., Doty, B., Dirmeyer, P., Adams, J., Mitchell, K., Wood, E. F., and Sheffield, J.: Land
676 information system: An interoperable framework for high resolution land surface modeling,
677 *Environmental Modelling & Software*, 21, 1402–1415,
678 <https://doi.org/10.1016/j.envsoft.2005.07.004>, 2006.
- 679 Kumar, S. V., Peters-Lidard, C. D., Santanello, J., Harrison, K., Liu, Y., and Shaw, M.: Land
680 surface Verification Toolkit (LVT) – a generalized framework for land surface model evaluation,
681 *Geosci. Model Dev.*, 5, 869–886, <https://doi.org/10.5194/gmd-5-869-2012>, 2012.
- 682 Kumar, S. V., Peters-Lidard, C. D., Mocko, D., and Tian, Y.: Multiscale Evaluation of the
683 Improvements in Surface Snow Simulation through Terrain Adjustments to Radiation, 14, 220–232,
684 <https://doi.org/10.1175/JHM-D-12-046.1>, 2013.
- 685 Ma, Z., Xu, J., Zhu, S., Yang, J., Tang, G., Yang, Y., Shi, Z., and Hong, Y.: AIMERG: a new Asian
686 precipitation dataset (0.1°/half-hourly, 2000–2015) by calibrating the GPM-era IMERG at a daily
687 scale using APHRODITE, 12, 1525–1544, <https://doi.org/10.5194/essd-12-1525-2020>, 2020.
- 688 Manz, B., Páez-Bimos, S., Horna, N., Buytaert, W., Ochoa-Tocachi, B., Lavado-Casimiro, W., and
689 Willems, B.: Comparative Ground Validation of IMERG and TMPA at Variable Spatiotemporal
690 Scales in the Tropical Andes, 18, 2469–2489, <https://doi.org/10.1175/JHM-D-16-0277.1>, 2017.
- 691 McNally, A.: GES DISC Dataset: FLDAS Noah Land Surface Model L4 Global Monthly 0.1 x 0.1
692 degree (MERRA-2 and CHIRPS) (FLDAS_NOAH01_C_GL_M 001), 2018.



- 693 McNally, A., Husak, G. J., Brown, M., Carroll, M., Funk, C., Yatheendradas, S., Arsenault, K.,
694 Peters-Lidard, C., and Verdin, J. P.: Calculating Crop Water Requirement Satisfaction in the West
695 Africa Sahel with Remotely Sensed Soil Moisture, *J. Hydrometeor.*, 16, 295–305,
696 <https://doi.org/10.1175/JHM-D-14-0049.1>, 2015.
- 697 McNally, A., Shukla, S., Arsenault, K. R., Wang, S., Peters-Lidard, C. D., and Verdin, J. P.:
698 Evaluating ESA CCI soil moisture in East Africa, *International Journal of Applied Earth
699 Observation and Geoinformation*, 48, 96–109, <https://doi.org/10.1016/j.jag.2016.01.001>, 2016.
- 700 McNally, A., Arsenault, K., Kumar, S., Shukla, S., Peterson, P., Wang, S., Funk, C., Peters-lidard,
701 C. D., and Verdin, J. P.: A land data assimilation system for sub-Saharan Africa food and water
702 security applications, 4, 170012, <http://dx.doi.org/10.1038/sdata.2017.12>, 2017.
- 703 McNally, A., McCartney, S., Ruane, A. C., Mladenova, I. E., Whitcraft, A. K., Becker-Reshef, I.,
704 Bolten, J. D., Peters-Lidard, C. D., Rosenzweig, C., and Uz, S. S.: Hydrologic and Agricultural
705 Earth Observations and Modeling for the Water-Food Nexus, *Front. Environ. Sci.*, 7,
706 <https://doi.org/10.3389/fenvs.2019.00023>, 2019.
- 707 Record Low Snowpack in Afghanistan: [https://earthobservatory.nasa.gov/images/91851/record-low-](https://earthobservatory.nasa.gov/images/91851/record-low-snowpack-in-afghanistan)
708 [snowpack-in-afghanistan](https://earthobservatory.nasa.gov/images/91851/record-low-snowpack-in-afghanistan), last access: 20 March 2018.
- 709 NASA JPL: NASA Shuttle Radar Topography Mission Global 30 arc second [Data set]. NASA
710 EOSDIS Land Processes DAAC, NASA EOSDIS Land Processes DAAC, NASA EOSDIS Land
711 Processes DAAC., 2013.
- 712 Nazemosadat, M. J. and Ghaedamini, H.: On the Relationships between the Madden–Julian
713 Oscillation and Precipitation Variability in Southern Iran and the Arabian Peninsula: Atmospheric
714 Circulation Analysis, 23, 887–904, <https://doi.org/10.1175/2009JCLI2141.1>, 2010.
- 715 NCAR Research Applications Library: <https://ral.ucar.edu/solutions/products/unified-noah-lsm>, last
716 access: 12 November 2021.
- 717 Nguyen, P., Thorstensen, A., Sorooshian, S., Hsu, K., Aghakouchak, A., Ashouri, H., Tran, H., and
718 Braithwaite, D.: Global Precipitation Trends across Spatial Scales Using Satellite Observations, 99,
719 689–697, <https://doi.org/10.1175/BAMS-D-17-0065.1>, 2018.
- 720 Niu, G.-Y., Yang, Z.-L., Mitchell, K. E., Chen, F., Ek, M. B., Barlage, M., Kumar, A., Manning, K.,
721 Niyogi, D., Rosero, E., Tewari, M., and Xia, Y.: The community Noah land surface model with
722 multiparameterization options (Noah-MP): 1. Model description and evaluation with local-scale
723 measurements, 116, <https://doi.org/10.1029/2010JD015139>, 2011.
- 724 NOAA: [https://www.climate.gov/news-features/blogs/enso/september-enso-update-la-ni%C3%B1a-](https://www.climate.gov/news-features/blogs/enso/september-enso-update-la-ni%C3%B1a-watch)
725 [watch](https://www.climate.gov/news-features/blogs/enso/september-enso-update-la-ni%C3%B1a-watch), last access: 12 September 2017.



- 726 NOAA CPC ENSO Cold & Warm Episodes by Season:
727 https://origin.cpc.ncep.noaa.gov/products/analysis_monitoring/ensostuff/ONI_v5.php, last access:
728 29 July 2021.
- 729 Oki, T. and Kanae, S., S.: Global Hydrological Cycles and World Water Resources, *Science*, 313,
730 1068–1072, <https://doi.org/10.1126/science.1128845>, 2006.
- 731 Pervez, S., McNally, A., Arsenault, K., Budde, M., and Rowland, J.: Vegetation Monitoring
732 Optimization With Normalized Difference Vegetation Index and Evapotranspiration Using Remote
733 Sensing Measurements and Land Surface Models Over East Africa, 3, 1,
734 <https://doi.org/10.3389/fclim.2021.589981>, 2021.
- 735 Peters-Lidard, C. D., Houser, P. R., Tian, Y., Kumar, S. V., Geiger, J., Olden, S., Lighty, L., Doty,
736 B., Dirmeyer, P., Adams, J., Mitchell, K., Wood, E. F., and Sheffield, J.: High-performance Earth
737 system modeling with NASA/GSFC’s Land Information System, *Innovations Syst Softw Eng*, 3,
738 157–165, <https://doi.org/10.1007/s11334-007-0028-x>, 2007.
- 739 Qamer, F. M., Tadesse, T., Matin, M., Ellenburg, W. L., and Zaitchik, B.: Earth Observation and
740 Climate Services for Food Security and Agricultural Decision Making in South and Southeast Asia,
741 100, ES171–ES174, <https://doi.org/10.1175/BAMS-D-18-0342.1>, 2019.
- 742 Rana, S., Renwick, J., McGregor, J., and Singh, A.: Seasonal Prediction of Winter Precipitation
743 Anomalies over Central Southwest Asia: A Canonical Correlation Analysis Approach, *J. Climate*,
744 31, 727–741, <https://doi.org/10.1175/JCLI-D-17-0131.1>, 2018.
- 745 Rodell, M., Famiglietti, J. S., Wiese, D. N., Reager, J. T., Beaudoin, H. K., Landerer, F. W., and
746 Lo, M.-H.: Emerging trends in global freshwater availability, 557, 651,
747 <https://doi.org/10.1038/s41586-018-0123-1>, 2018.
- 748 Sarmiento, D. P., Slinski, K., McNally, A., Funk, C., Peterson, P., and Peters-Lidard, C. D.: Daily
749 precipitation frequency distributions impacts on land-surface simulations of CONUS, *Front. Water*,
750 0, <https://doi.org/10.3389/frwa.2021.640736>, 2021.
- 751 Schiemann, R., Lüthi, D., Vidale, P. L., and Schär, C.: The precipitation climate of Central Asia—
752 intercomparison of observational and numerical data sources in a remote semiarid region, 28, 295–
753 314, <https://doi.org/10.1002/joc.1532>, 2008.
- 754 Shukla, S., Arsenault, K. R., Hazra, A., Peters-Lidard, C., Koster, R. D., Davenport, F., Magadzire,
755 T., Funk, C., Kumar, S., McNally, A., Getirana, A., Husak, G., Zaitchik, B., Verdin, J., Nsadisa, F.
756 D., and Becker-Reshef, I.: Improving early warning of drought-driven food insecurity in southern
757 Africa using operational hydrological monitoring and forecasting products, 20, 1187–1201,
758 <https://doi.org/10.5194/nhess-20-1187-2020>, 2020.



- 759 Shukla, S., Landsfeld, M., Anthony, M., Budde, M., Husak, G. J., Rowland, J., and Funk, C.:
760 Enhancing the Application of Earth Observations for Improved Environmental Decision-Making
761 Using the Early Warning eXplorer (EWX), 2, 34, <https://doi.org/10.3389/fclim.2020.583509>, 2021.
- 762 Tan, J., Petersen, W. A., and Tokay, A.: A Novel Approach to Identify Sources of Errors in IMERG
763 for GPM Ground Validation, 17, 2477–2491, <https://doi.org/10.1175/JHM-D-16-0079.1>, 2016.
- 764 500,000 children affected by drought in Afghanistan – UNICEF: [https://www.unicef.org/press-](https://www.unicef.org/press-releases/500000-children-affected-drought-afghanistan-unicef)
765 [releases/500000-children-affected-drought-afghanistan-unicef](https://www.unicef.org/press-releases/500000-children-affected-drought-afghanistan-unicef), last access: 23 April 2018.
- 766 USGS Knowelge Base:
767 <https://earlywarning.usgs.gov/fews/searchkb/Asia/Central%20Asia/Afghanistan>, last access: 12
768 November 2021.
- 769 Verdin, A., Funk, C., Peterson, P., Landsfeld, M., Tuholske, C., and Grace, K.: Development and
770 validation of the CHIRTS-daily quasi-global high-resolution daily temperature data set, *Sci Data*, 7,
771 303, <https://doi.org/10.1038/s41597-020-00643-7>, 2020.
- 772 Xie, P. and Arkin, P. A.: Analyses of Global Monthly Precipitation Using Gauge Observations,
773 Satellite Estimates, and Numerical Model Predictions, 9, 840–858, [https://doi.org/10.1175/1520-](https://doi.org/10.1175/1520-0442(1996)009<0840:AOGMPU>2.0.CO;2)
774 [0442\(1996\)009<0840:AOGMPU>2.0.CO;2](https://doi.org/10.1175/1520-0442(1996)009<0840:AOGMPU>2.0.CO;2), 1996.
- 775 Yatagai, A., Kamiguchi, K., Arakawa, O., Hamada, A., Yasutomi, N., and Kitoh, A.: APHRODITE:
776 Constructing a Long-Term Daily Gridded Precipitation Dataset for Asia Based on a Dense Network
777 of Rain Gauges, 93, 1401–1415, <https://doi.org/10.1175/BAMS-D-11-00122.1>, 2012.
- 778 Yoon, Y., Kumar, S. V., Forman, B. A., Zaitchik, B. F., Kwon, Y., Qian, Y., Rupper, S., Maggioni,
779 V., Houser, P., Kirschbaum, D., Richey, A., Arendt, A., Mocko, D., Jacob, J., Bhanja, S., and
780 Mukherjee, A.: Evaluating the Uncertainty of Terrestrial Water Budget Components Over High
781 Mountain Asia, 7, 120, <https://doi.org/10.3389/feart.2019.00120>, 2019.

782